“Hexagonal” Perovskites – From Stacking Sequence to Space Group Symmetry and New Opportunities

Sylvia L. Kunz[a], Michael Haefner[b], Oliver Clemens[a,*]

[a] University of Stuttgart, Institute for Materials Science, Materials Synthesis Group, Heisenbergstraße 3, 70569 Germany

[b] Bavarian Center for Battery Technology (BayBatt), University of Bayreuth, Weiherstrasse 26, 95448 Bayreuth, Germany

* Corresponding Author:

Prof. Dr. Oliver Clemens

Email: oliver.clemens@imw.uni-stuttgart.de

Fax: +49 711 685 51933

Abstract

The term hexagonal perovskite has been widely used in literature to discuss the structure of perovskite-type compounds with composition ABX_{3-y} with partial h-type stacking of AX_3 layers. Though the local surrounding of these AX_3 layers resembles a hexagonal close packing, the space group symmetries reported for some of these materials are not belonging to the hexagonal crystal system, but are trigonal or orthorhombic instead. Though reports and books with lists of hexagonal perovskites exist which assign stacking sequences and list a corresponding space group together with them, a concise guideline on how the symmetry of the perovskite type material is related to the stacking sequence has not been reported. Clearly, such a systematization of space group symmetry and stacking notations would be desirable – for distortion or ordering variants of the cubic perovskite, the whole research community benefits from concepts of group-subgroup relations or classification of tilting via the Glazer notation.

In this article, we derive a fully consistent guideline on how the aristotype space group symmetry can be determined for any stacking sequence (e.g., cchhchcch…) in the Jagodzinski notation and provide a computer program which can do this analysis. By this, one can narrow down the possible aristotype space group symmetries for any perovskite stacking sequence with h-type layers to seven space groups in total ($R\text{-}3m$, $P\text{-}3m$, $P6_3/mmc$, $P\text{-}6m2$, $R3m$, $P3m$, and $P6_3mc$), and the space groups can be directly derived from the Jagodzinski sequence. Remarkably, the possibility to obtain polar perovskites with h-type layers by stacking has not been recognized in literature so far, and provides the opportunity to develop new multiferroic materials by design of stacking.

Keywords

Stacking sequence; Hexagonal Perovskites; Pyrolectrics; Multiferroics; Symmetry Analysis

1 Introduction

The term “perovskite” was introduced in 1839 by the German mineralogist Gustave Rose to denote the mineral $CaTiO_3$. It was named after Lew Alexejewitsch Perowski, a russian politician and mineralogist. Meanwhile, the term “perovskite” is more widely used for the structure type family with the general sum formula ABX_3. Perovskites are renowned for their structural and compositional flexibility which exhibits variations on both the cation A [1-3] and B cation [4, 5], as well as on the anion sublattice [2, 6-11]. The huge variety of possible chemical compositions within these materials enables to customize chemical properties for specific applications such as oxygen permeable membranes, cathode materials for intermediate temperature solid oxide fuel cells ($Ba_xSr_{1-x}Co_{1-y}Fe_yO_{3-\delta}$) [12], solar cells [13], light emitting diodes (LED) [14], transistors [15], and as catalyst [16], to name only a few.

Due to the high diversity within the perovskite structure type family, numerous different crystal structures have been reported, which are well-summarized in the book from Tilley [17]. The most well-known perovskite-type structure ABX_3 is cubic and crystalizes in the space group *Pm*-3*m* *w*ith a lattice parameter ~ 3.9 ($SrTiO_3$ [18]) - 4.5 Å [19]. In this cubic perovskite, the octahedra [BX_6] share corners with 180 ° X-B-X bond angles, while *A* is surrounded by 12 *X* anions, forming a cuboctahedron [AX_{12}]. As an alternative, the [BX_6] octahedra chains can also be connected via face-sharing, resulting in a so-called “hexagonal” perovskite with symmetry $P6_3/mmc$. In addition, a combination of both, corner- and face-sharing between the octahedra is possible. The different connectivity results from a different stacking of AX_3 layers and the underlying filling of octahedral sites by B therein. These perovskites with at least partial face sharing of BX_6 octahedra are then also often referred to as “hexagonal” perovskites, though some of them do not appear to crystallize in the hexagonal crystal system with space groups such as *P*-3*m* [20], or *R*-3*m* [6] or even orthorhombic [21] compounds; thus the naming is referring more to the fact that some building blocks resemble the situation in a hexagonal close packing, and do not relate to the crystal symmetry directly.

Since such “hexagonal” perovskites can also be described by a stacking sequence in Jagodzinski notation (e.g., chcch; these notations will be explained in the course of manuscript for the reader unfamiliar with it), it is common to refer to certain hexagonal perovskites by a combination of a number and a capital letter. The number refers to the number of ABX_3 stacking folds required to describe the length of the unit cell along the stacking direction, and the letter somehow refers to the crystal system or Bravais Lattice. For example, the hexagonal perovskite with hh stacking sequence, two stacks of ABX_3 within the unit cell and a symmetry of $P6_3/mmc$ is referred to as 2H perovskite; the cubic perovskite with space group *Pm*-3*m* contains three stacking folds along the $[1\ 1\ 1]_{cub}$ direction and is thus referred to as 3C perovskite. In many instances, when hexagonal and cubic stacking sequences are combined, the space group $P6_3/mmc$ is obtained (4H, 6H, 8H, etc.) or the space group R-3m (9R, 15R, etc.). However, these labels are not always used consistently in literature, and compounds with a symmetry of P-3m have also been referred to as 5H perovskites or hexagonal perovskites [20], though they are described in the trigonal crystal system.

On inspecting lists of "hexagonal perovskite" materials as e.g. given in the book of Tilley [17], it remains rather non-intuitive which space group must be assigned to a specific stacking sequence and why this is the case. From reading through many textbooks on perovskites and structural chemistry, this aspect did not become clear to the authors of this article either way. Thus, we think it is worth developing a more intuitive and conceptional understanding on these stacking sequences and what symmetry must / can result from them. Such symmetry considerations are well developed for perovskite materials related to the cubic aristotype (tilting variants and ordering variants) and very helpful, and next to space group analysis with group-subgroup relations [22] there are also concepts easier to visualize in someone's mind, e.g., the Glazer notation [23].

In the present work we will show that the aristotype symmetry of different stacking sequences can be easily derived following a few very simple rules, which can be derived from considerations of local symmetry on A- and B-site cations and how these local site symmetries can be arranged in space to obtain a final space group. This requires a rather long argumentation chain, which we proceed through step by step. To make the article understandable to readers not entirely familiar with concepts of stacking notation, we tried to explain the notations used whenever we thought this could be helpful to avoid confusions. From the rules derived, we will provide insights on which perovskite materials with h-type layers are already known and which are yet to be explored, which materials possess aristotype symmetry and for which the maximum symmetry of the stacking is further broken. We will show that polar materials with related potential multiferroic properties could become possible within polarly stacked sequences (similar to other layered perovskites with Dion-Jacobson-type structure [24]), highlighting a pathway for making new multiferroic materials with exciting new functionalities [25].

2 Results and Discussions

2.1 Perovskite compositions ABX_3, close packing of AX_3 layers and occupation of octahedral sites by B cations

The term "perovskite" has been used to describe various materials with similar structural arrangements and compositions. For the considerations described below, it is important to define what we will consider as a perovskite-type compound / material. Let us begin our discussion by defining the structural motif that unites all perovskite-type compounds mentioned in the following sections. For this we define a perovskite-type compound as a crystalline solid material with a composition ABX_3, where X is an anion, A is a large cation approximately the size as the X anion, and B is a smaller cation that fits into an octahedron formed by the six X anions. In every perovskite material, one finds a substructure which is derived from a close packing of AX_3. Distinguishable sequences of stacking result in different aristotype structures of perovskite materials. In this close packing, the B cations fill all the octahedral sites only connected to X anions, forming $[BX_6]$ octahedra. Further, the A cations are surrounded by twelve X anions, arranged either in a cuboctahedron or an anti-cuboctahedron coordination $[AX_{12}]$.

In the following, we will explain how the maximum symmetry of the individual aristotypes can be derived based on the stacking sequence. This requires a long chain of reasoning, which we will develop in the following sections.

This chain of reasoning includes the derivation of maximum point group symmetry of the *A*- and *B*- site cations based on their position within the stacking sequence, the determination of a suitable unit cell depending on (or independent of) the stacking sequence, the importance of centering and screw axes in relation to the stacking sequence, and the identification of space groups compatible with the maximum point group symmetry.

To obtain the maximum symmetry, we simplify our perovskite model to the hypothetical (but useful) scenario where A and X are hard spheres of identical radii, $r(A) = r(X)$, and that the B cations are hard spheres that fit perfectly into the octahedral gaps formed by the X-anions, i.e., $r(B) = ((\sqrt{2})-1)\ r(X)$. In this scenario, the construction of the unit cell can be done to maximize the density of the compound. For this the atomic nuclei of the atoms within an AX_3 layer must align within a plane. Further, if we draw normals perpendicular to these planes, one can only find either cations (A- and B-site) or X anions lying on the respective lines. In addition, the maximization of density by packing hard spheres automatically results in high symmetry of AX_{12} and BX_6 polyhedra of the first coordination sphere (as we will discuss later). This high symmetry will only be broken considering the higher order coordination spheres.

One can now derive structural scenarios, which agree with the definition of “perovskite” given above. First, let us examine the structure of a single close packed AX_3 layer. To achieve a layer composition of AX_3 without any A-A contacts, lines of composition X must be alternated with lines of $A_{1/2}X_{1/2}$ (see Figure 1). In this arrangement, every A cation is surrounded by 6 X anions; likewise, every X anion is surrounded by 4 X anions and 2 A cations.

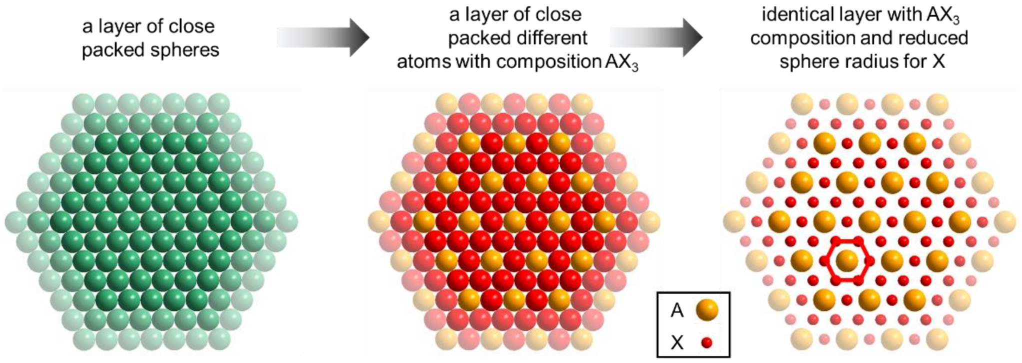

Figure 1. Derivation of a close packed layer of composition AX_3 from a close packed layer of spheres.

To ensure the *A* cation is only surrounded by the *X* anions, one can consider how a second close packed AX_3 layer can be positioned on top of our original AX_3 layer. Hence, one can identify triangles within the AX_3 layers formed by 3 *X* anions, as shown in Figure 2. In this figure, some triangles (green) point “upwards”, while other (blue) point “downwards”. Each pattern of triangles has the same orientation as the *A* sublattice of the AX_3 layer; therefore, a second layer can either be placed on top of either the blue triangles or the green triangles. These orientations are indicated by “recoloring” the corresponding atoms of the AX_3 layers stacked onto the original layer.

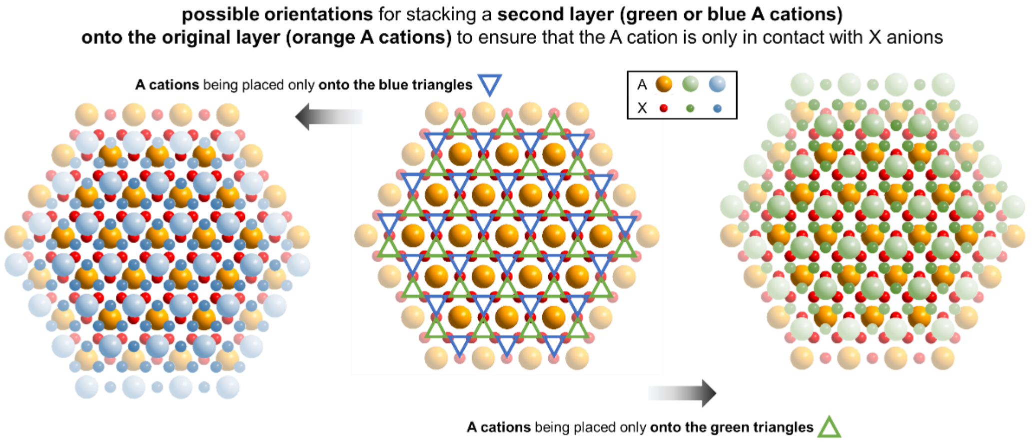

Figure 2. Possible orientations for stacking a second layer (green or blue A cations) onto the original layer (orange A cations) to ensure that the A cation is only in contact with X anions.

Now, to achieve the 12-fold coordination of *A* cations by *X* anions as described in the above definition, a third close-packed layer is placed below the original layer of the double stacks. Since the *A* cations of this third layer are only directly interacting with the *X* anions of the original layer, this third layer can be placed below either the blue or the green triangles. This results in triple stacks, as indicated Figure 3. The resulting coordination environments of the A cations of the original layer are a cuboctahedron when sandwiched between a green and a blue layer, or an anti-cuboctahedron when sandwiched between two green or between two blue layers. The fact that we performed the stacking under the condition of maximum density with $r(A) = r(X)$ implies that the symmetry of the first coordination sphere is the highest symmetry possible for this individual coordination polyhedron, again see Figure 3).

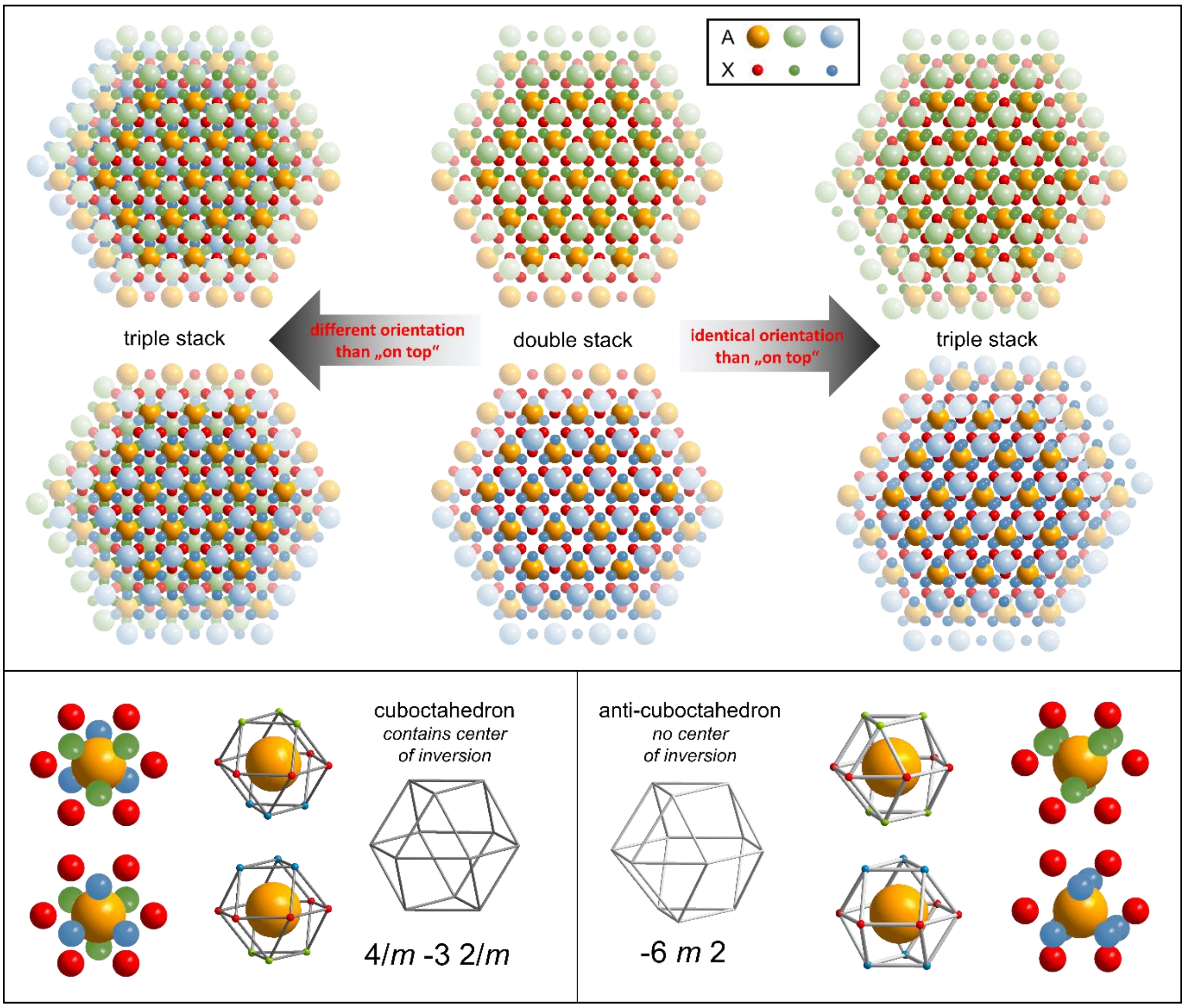

possible orientations for stacking **a third layer** (green or blue A cations) **below the original layer** (orange A cations) to ensure that the A cations of the original layer are surrounded by 12 X anions

Figure 3. Possible orientations for stacking a third layer (green or blue A cations) below the original layer (orange A cations) to ensure that the A cations of the original layer are surrounded by 12 X anions.

The stacking can also be represented using the well-known description of stacking sequences *A*, *B*, and *C*, as there are only three possible orientations of the AX_3 layers along the direction of stacking. Thus, the green-orange-blue scenario is described by the three-letter sequence *ABC* (or one of the permutations *CBA*, *BAC*, *CAB*, *BCA*, *ACB*), and the blue-orange-blue or green-orange-green scenarios are described by the sequence *ABA* (or one of the permutations *CBC*, *BAB*, *CAC*, *ACA*, *BCB*). For our later discussion, it will also be relevant to introduce a different notation for describing the stacking sequence using only two letters: *c* (for cubic) and *h* (for hexagonal). This notation is called Jagodzinski notation, and is easily derived from the aforementioned sequence based on the letters *A*, *B*, and *C*. If a layer is surrounded by two identical letters, it is described as “*h*”, whereas if it is surrounded by two different letters, it is described as “*c*”. Figure 4 shows an example of an arbitrary excerpt of a sequence of layers along with the Jagodzinski notation derived from it.

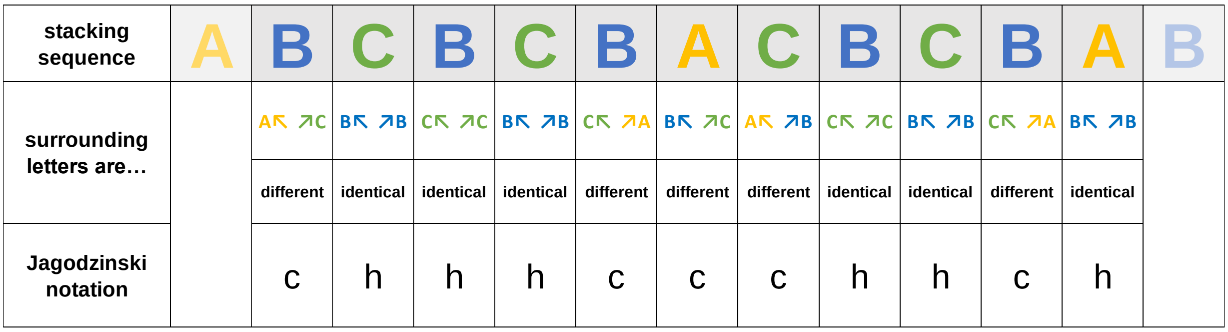

stacking sequence	A	B	C	B	C	B	A	C	B	C	B	A	B
surrounding letters are…		A↖ ↗C	B↖ ↗B	C↖ ↗C	B↖ ↗B	C↖ ↗A	B↖ ↗C	A↖ ↗B	C↖ ↗C	B↖ ↗B	C↖ ↗A	B↖ ↗B	
		different	**identical**	**identical**	**identical**	**different**	**different**	**different**	**identical**	**identical**	**different**	**identical**	
Jagodzinski notation		c	h	h	h	c	c	c	h	h	c	h	

Figure 4. Scheme illustrating how to derive the corresponding Jagodzinski notation from an excerpt of a randomly chosen stacking sequence in ABC notation.

The Jagodzinski notation is well-suited for easily describing all possible stacking patterns of AX_3 layers in perovskite materials. For any crystal as a 3-dimensional periodic arrangement, it is necessary for the stacking sequence to repeat after a certain length.

We therefore note at this state: every distinguishable and unique stacking pattern (which cannot be transformed into another one by changing the choice of the origin) results in an individual aristotype perovskite compound. We emphasize that this is a difference to the many lower symmetry tilt modifications [26] or ordering variants of the cubic perovskite, which can all be related to the cubic aristotype compound via less or more complex group-subgroup relations [22].

For instance, the stacking sequence $(chc)_\infty$ is equivalent to the stacking sequences $(cch)_\infty$ and $(hcc)_\infty$, but it differs from the stacking sequences $(ccch)_\infty$ and $(hhc)_\infty$. We can further add the rather trivial statement that any stacking other than the pure c_∞ stacking will contain *h*-type layers. The pure c_∞ stacking sequence results in the cubic perovskite.

Let us now examine the orientation of the different symmetry elements of the first coordination sphere of the *A*-cations. These symmetry elements are shown in Figure 5. We note that the anti-cuboctahedron only possesses symmetry elements which are perpendicular to or along the direction of stacking. This has a very important implication: all symmetry elements for the cuboctahedron that are not perpendicular to or along the direction of stacking or contain the direction of stacking, will be lost if an *h*-type layer exists within the stacking sequence. One can visualize this by understanding that the 4-fold rotational axes are forbidden to penetrate *h*-type layers (since there is no position within the plane which is compatible with this symmetry operation), while the 3-fold rotational axes run perpendicular to *h*-type layers. In other words: only the c_∞ infinity stacking sequence corresponding to the cubic aristotype perovskite will permit the highest symmetry of the cuboctahedron, which will then be 4/*m* -3 2/*m*. All stacking sequences of the other aristotypes containing *c*- and h-type layers will induce a maximum symmetry of the cubocotahedron of -3 2/*m.* Additionally, since the symmetry of the anti-cuboctahedron is not affected by the presence of a c-type layer in general (3-fold rotation axes within a single AX_3 layer are not only running through the A cations, but also through the center of gravity of the triangles formed by X anions), and thus the maximum possible symmetry of the anti-cuboctahedron remains -6 *m* 2 (again, see Figure 5).

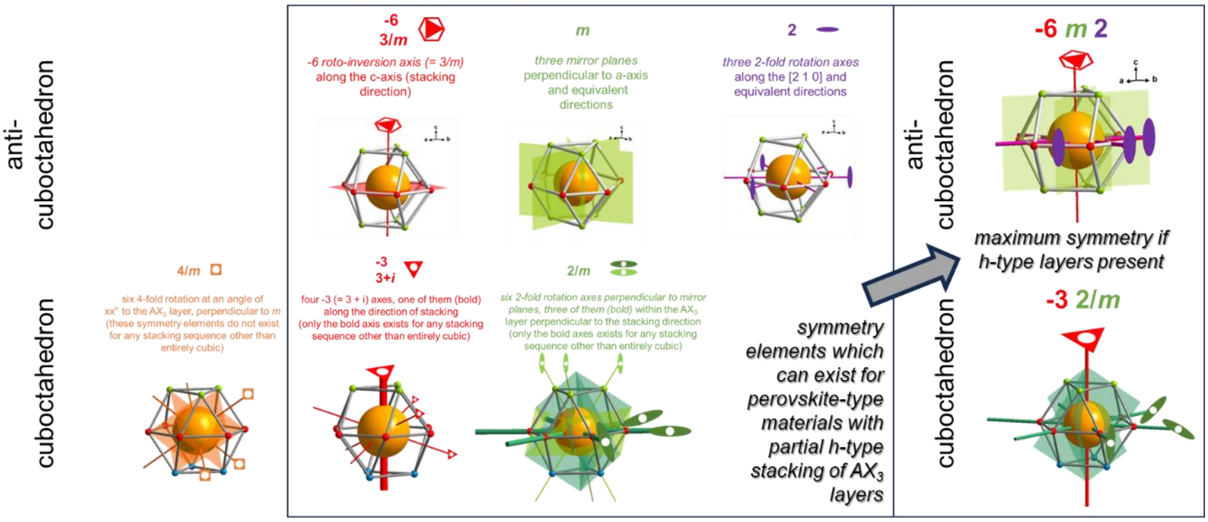

Figure 5. From highest polyhedron symmetry of the A-cations to the maximum polyhedron symmetry on the presence of h-type layers.

We also observe from Figure 5 that while the cuboctahedron has a center of symmetry / inversion center at the *A* cation of the original layer, it does not possess a mirror plane perpendicular to the stacking direction. In contrast, the anti-cuboctahedron does not have a center of symmetry. However, in this case, a mirror plane exists perpendicular to the stacking direction, containing *A*- and *X*-type ions. This is implicitly given by the -6 roto-inversion axis perpendicular to the layer stack, which does not contain a center of symmetry but implies a 3-fold rotation axis running perpendicular to the mirror stack and a mirror plane within the central layer of the layer stack (3/*m*)).

To achieve our goal of determining the maximum space group symmetry for individual non-equivalent stacking sequences representing the different aristotypes, it is not sufficient to focus only on the *A* cations of the close packed AX_3 layers. We further need to consider the position of the *B* cations between two layers. We begin by examining a two-layer stack (see Figure 6), and identify octahedrally coordinated sites in the middle between the two layers formed by 6 *X* anions; these can be filled by the B cations. Since we observe that the areal number density of such sites is ¼ of the areal number density of close packed spheres within one layer (or equivalently, identical to the areal density of AX_3 units within a close packed layer), stacking

AX_3 layers and filling the X_6 octahedral gaps between the layers by B cations yields an overall composition of ABX_3, consistent with the definition provided earlier. The highest symmetry of an octahedron is $4/m$ -3 $2/m$; the 4-fold rotational axes are oriented at an angle of ~ 35.26 ° with respect to the AX_3 layers, the -3 axis is oriented perpendicular to the AX_3 layers along the direction of stacking and the 2-fold axis lies parallel to the AX_3 layers and runs through two opposite edges of the octahedron. For maximized density, the symmetry of the first coordination sphere of the ocrtahedron is $4/m$ -3 $2/m$, but the 4-fold symmetry must again be lost if a single h-type layer will be present. Taking this into account the maximum symmetry when considering higher order coordination spheres in the presence of a single h-type layer will be reduced to at least -3 $2/m$.

For the later discussion, special attention must be given to the 3-fold roto-inversion axis "–3", which runs along the stacking direction (all other -3 axes cannot exist in the presence of a single h-type layer, basically for the same reason as 4-fold symmetry cannot exist any more) and perpendicular to the AX_3 layers. This symmetry operation implies the existence of a proper 3-fold rotation axis running through the B cation and a center of symmetry at the position of the B cation.

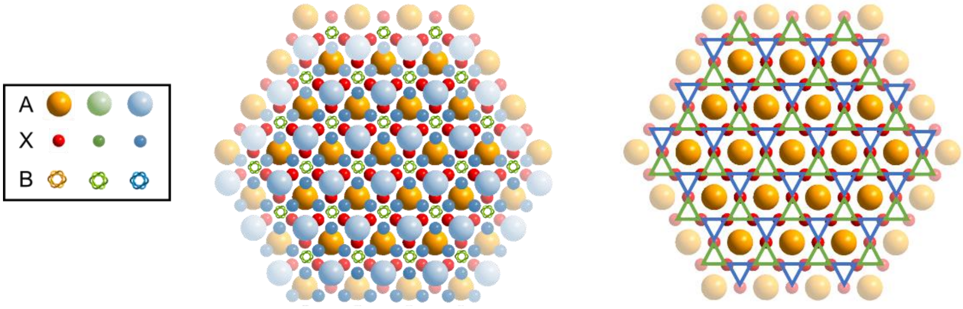

Figure 6. Orientation of the B cation sites within X_6 octahedral gaps between two close packed AX_3 layers.

Now, let us take a closer look at the position of the B cations. By examining Figure 6, we find that the B cations occupy the position in the center of the green triangles. This can be transferred to the *ABC* notation of our stacking sequence, by assigning the Greek letters α, β, and γ to these octahedral sites, to relate their positions to the orientation of the close packed layers *A*, *B*, and *C*, respectively. Since the octahedral sites are only occupied by one quarter, their position and filling in any stacking sequence can now be described according to the scheme shown in Figure 7. It is also worth noting that the B cations, for example in a $\gamma_{1/4}$ layer, have the same orientation within the layer as the A cations do in a C layer. This observation will become important later when we want to derive the maximum rotational symmetry (existence of rotation, roto inversion or screw axes). Furthermore, we note that the BX_6 octahedra within one layer are isolated from each other; they do not share a common face, edge or corner of the octahedron.

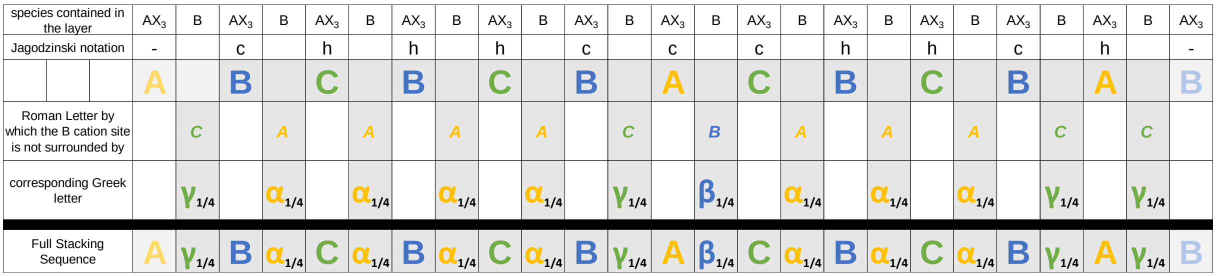

species contained in the layer	AX_3	B	AX_3	B	AX_3	B	AX_3	B	AX_3	B	AX_3	B	AX_3	B	AX_3	B	AX_3	B	AX_3	B	AX_3	B	AX_3	B	AX_3
Jagodzinski notation	-		c		h		h		h		c		c		c		h		h		c		h		-
	A		B		C		B		C		B		A		C		B		C		B		A		B
Roman Letter by which the B cation site is not surrounded by		*C*		*A*		*A*		*A*		*A*		*C*		*B*		*A*		*A*		*A*		*C*		*C*	
corresponding Greek letter		$\gamma_{1/4}$		$\alpha_{1/4}$		$\alpha_{1/4}$		$\alpha_{1/4}$		$\alpha_{1/4}$		$\gamma_{1/4}$		$\beta_{1/4}$		$\alpha_{1/4}$		$\alpha_{1/4}$		$\alpha_{1/4}$		$\gamma_{1/4}$		$\gamma_{1/4}$	
Full Stacking Sequence	A	$\gamma_{1/4}$	B	$\alpha_{1/4}$	C	$\alpha_{1/4}$	B	$\alpha_{1/4}$	C	$\alpha_{1/4}$	B	$\gamma_{1/4}$	A	$\beta_{1/4}$	C	$\alpha_{1/4}$	B	$\alpha_{1/4}$	C	$\alpha_{1/4}$	B	$\gamma_{1/4}$	A	$\gamma_{1/4}$	B

Figure 7. Scheme on how to derive the positions of the B cations within an excerpt of the randomly chosen stacking sequence given in Figure 4.

Now, we examine how the BX_6 octahedra are connected via an h-type or a c-type layer (see Figure 8). Though the BX_6 octahedra are isolated from each other within a bilayer stack of two AX_3 layers, they are connected to other octahedra in a different bilayer stack. While c-type layers result in a corner sharing of the octahedra with *B-X-B* angles of 180°, h-type layers connect ideal octahedra via faces with *B-X-B* angles of approximately 70.53°. By examining the structure perpendicular to the stacking direction, we observe that none of these double stackings disrupt the 3-fold rotational symmetry running through either the A or the B cations. Consequently, every individual orientation of the cations A/B/C/α/β/γ must always possess local 3-fold rotational symmetry at the respective Wyckoff site.

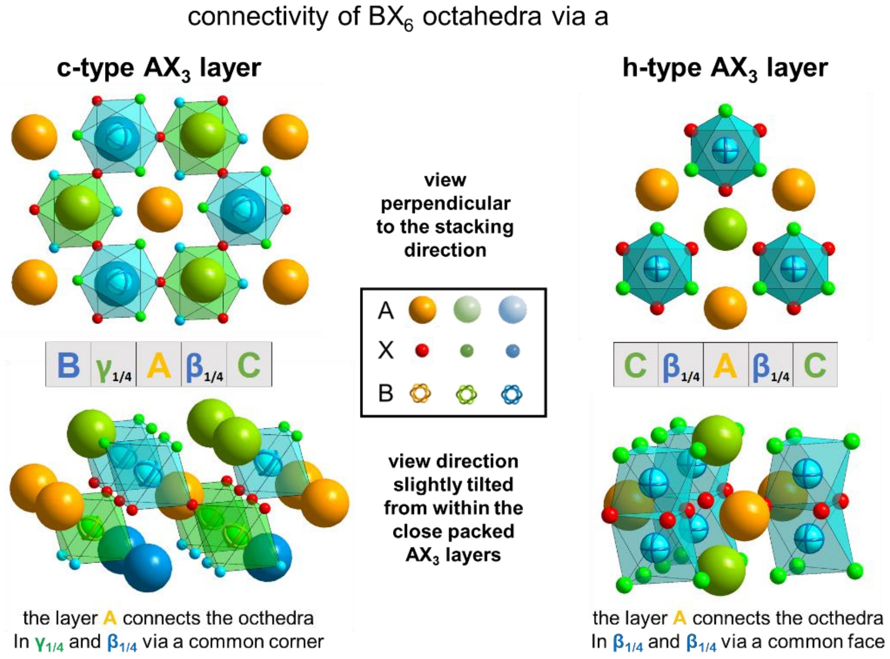

Figure 8. Connectivity of BX_6 octahedra via c-type and h-type layers.

Now, we need to examine if stacking can have an impact on the inversion symmetry, which is fundamentally present in an ideal cuboctahedron (observed for the *A* cations within a *c*-type AX_3 layer) as well as an ideal octahedron. Similarly, we need to examine the potential impact on stacking on the mirror symmetry of an anti-cuboctahedron around the *A* cation within an *h*-type AX_3 layer.

We will start with the octahedron, examining various stacking scenarios as illustrated in Figure 9, and discuss the three individual scenarios:

- Scenario 1 (Figure 9, left): The octahedron is connected to the octahedra of the two neighboring layers by a shared face to one side via an h-type AX_3 layer, and by sharing three corners to another side via a *c*-type AX_3 layer. The different connectivity to the opposite layers automatically results in the loss of the center of inversion on the *B* cation, with the only remaining symmetry element being the 3-fold rotation axis passing through the *B* cation perpendicular to the direction of stacking and the mirror planes perpendicular to the AX_3 layers. Put simply, when the *B* cation is situated between a *c*-type and an *h*-type layer, it cannot exhibit inversion symmetry. The resulting local symmetry on the B cations in the middle layer of the three octahedra layer stack is 3 *m*, and is consequently the maximum symmetry which a B-site cation in a ch local environment can have.
- Scenario 2 (Figure 9, middle): The octahedron is connected to the octahedra of the two neighboring layers by sharing of two opposite faces via two h-type AX_3 layers. This scenario can now in principle maintain the inversion symmetry on the B cation locally (further, the stacking sequence in one direction of stacking must also be invertible to the other direction, see later in this article). The resulting local symmetry on the B cations in the middle layer of the three octahedra layer stack is -3 2/*m*, and is consequently the maximum symmetry which a B-site cation in a “hh” local environment can have.
- Scenario 3 (Figure 9, right): The octahedron is connected to the octahedra of the two neighboring layers via corner sharing via two *c*-type AX_3 layers. In this scenario, it is theoretically possible to maintain inversion symmetry on the B cation locally. Additionally, the stacking sequence in one direction of stacking must also be invertible to the other direction, as we will explore later in this article. The resulting local symmetry on the B cations in the middle layer of the three octahedra layer stack is -3 2/*m*, and this is consequently the maximum symmetry which a B-site cation in a “cc” local environment can have.

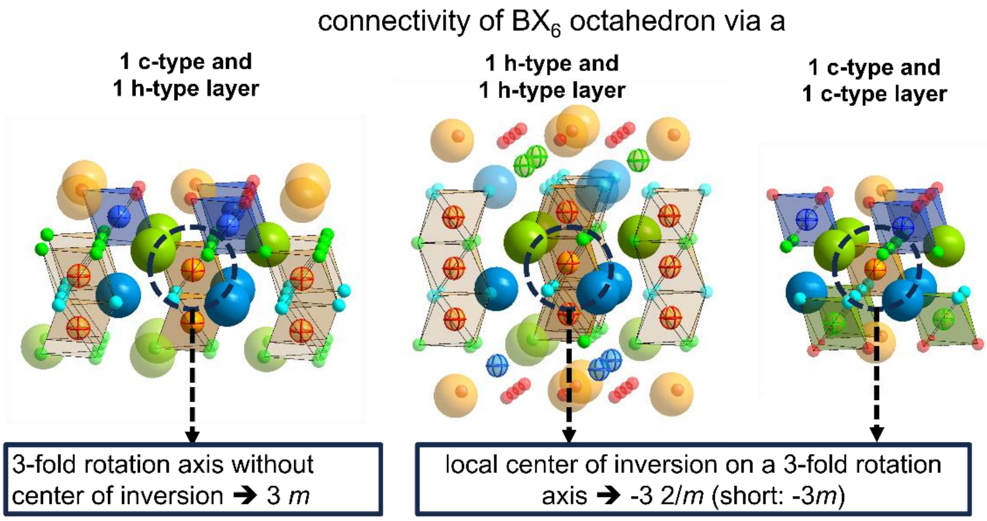

Figure 9. Local symmetry of octahedron connected via h-type and c-type layer (left), two h-type layers (middle), and two c-type layers (right).

Next, let us consider in an analogous way the conditions necessary to keep a center of symmetry on the *A* cation in a *c*-type layer (cuboctahedral coordination) or a mirror plane perpendicular to the 3-fold rotation axis on the *A* site cation in an *h*-type layer (anti-cuboctahedral coordination). It is evident that these symmetries are automatically broken if the layer is sandwiched between layers with different Jagodzinski symbols (see Figure 10). Thus, the above-mentioned symmetry elements do not exist for a cuboctahedron on a *c*-type layer between an *h*- and a *c*-type layer, as well as for an anti-cuboctahedron on an h-type layer between an *h*-type and a *c*-type layer. The resulting maximum local symmetry for both polyhedra is 3 *m, if the other viewing directions within the layer are also taken into account*. Without further discussion, we emphasize that the oxygen ions in a c- or h-type layer, for which the cation possesses local 3 *m* symmetry, will possess a local site symmetry of ". *m* .".

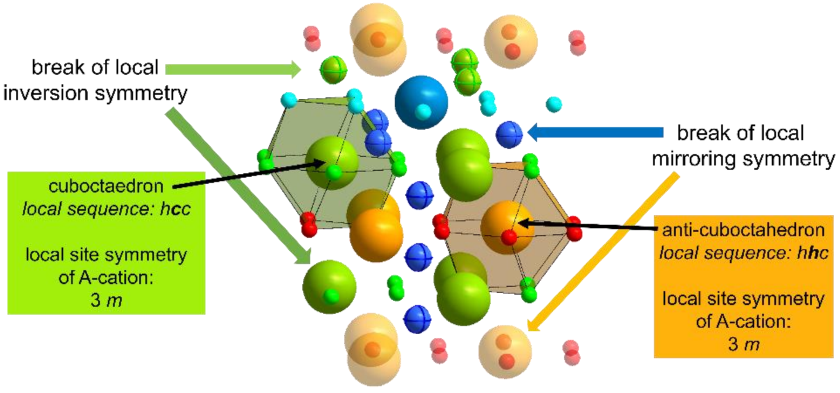

Figure 10. Loss of inversion of a cuboctahedron on a c-type layer between an h- and a c-type layer as well as loss of mirroring symmetry perpendicular to the direction of stacking for an anti-cuboctahedron on a h-type layer between an h-type and a c-type layer.

We increase the thickness of layer stacks to a five layer stack to see how a high symmetry on the A cations can be maintained. Similar as for the octahedron, we can visualize that it is possible to maintain the inversion symmetry for a cuboctahedron (which occurs in a c-type layer), if it is sandwiched within a five layer stack between two c-type layers (*c**c**c*) or between two h-type layers (*h**c**h*), see Figure 11, upper part. We note that these cuboctahedra in the middle of the five layer stack possess a local symmetry of -3 2/*m* (short -3 *m*), if viewing directions within the plane are also being considered. Without further discussion (we do not need to consider it further for the following discussions), we note that the oxygen ions in this c-type layer, for which the cation possesses local -3 *m* symmetry, will possess a local site symmetry of ". 2/*m* .".

Likewise, the anti-cuboctahedron can also maintain the mirroring symmetry perpendicular to the stacking direction, if it is sandwiched within a five layer stack between two c-type layers (*c**h**c*) or between two h-type layers (*h**h**h*), see Figure 11, lower part. Then, these anti-cuboctahedra in the middle of the five layer stack possess a local symmetry of -6 *m* 2 (reminder: -6 can be alternatively represented as 3/*m*), if the additional viewing directions are included. Without further discussion (we do not need to consider it further for the following discussions), we note that the oxygen ions in a h-type layer, for which the cation possesses local -6 *m* 2 symmetry, will possess a local site symmetry of "*m m* 2".

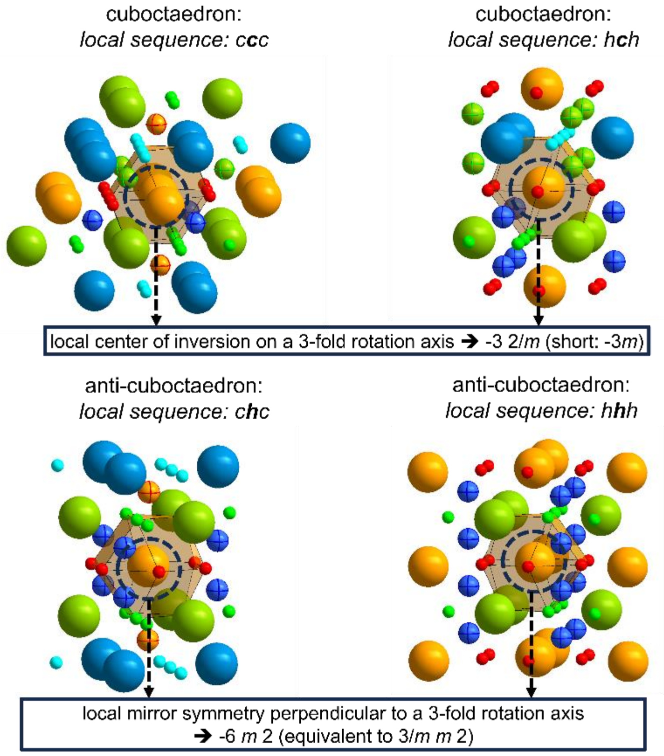

Figure 11. Local symmetries of cuboctahedron and anti-cuboctahedron surrounded by two h-type or two c-type layers.

So far, we have considered a more or less local picture for the symmetry of the A-site and B-site cations, since we have not considered the full stacking sequence and limited our considerations to the second (third) coordination spheres along the stacking direction. However, the understanding derived makes it now fairly straightforward to inspect the overall stacking sequence, which can destroy the inversion centers within a cuboctahedron / octahedron and lower the symmetry from -3 2/*m* to 3 *m*, or destroy the mirror plane within the anti-cuboctahedron perpendicular to the stacking direction, lowering the symmetry from -6 *m* 2 to 3 *m*. For this, we could inspect the full stacking sequence derivation of how to inspect the stacking sequence in the A/B/C/α/β/γ or Jagodzinski notation. The scheme on how to insect it is summarized and conceptionalized in Figure 12.

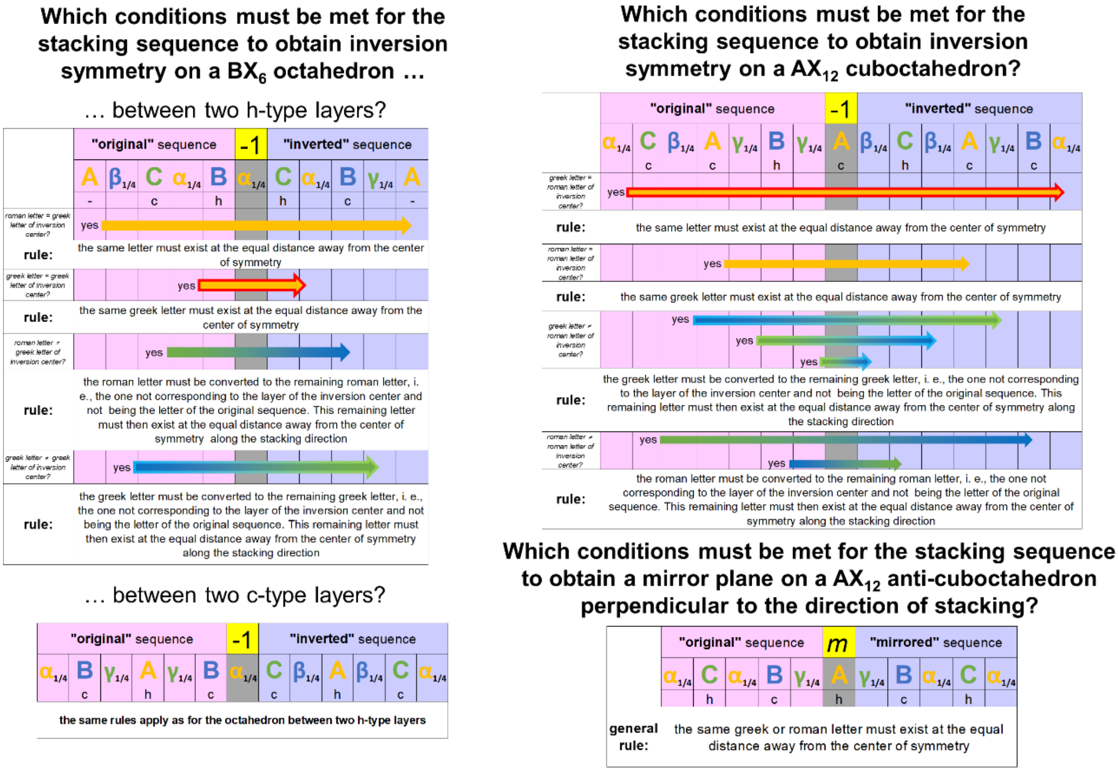
Which conditions must be met for the stacking sequence to obtain inversion symmetry on a BX_6 octahedron …

… between two h-type layers?

rule: the same letter must exist at the equal distance away from the center of symmetry

rule: the same greek letter must exist at the equal distance away from the center of symmetry

rule: the roman letter must be converted to the remaining roman letter, i. e., the one not corresponding to the layer of the inversion center and not being the letter of the original sequence. This remaining letter must then exist at the equal distance away from the center of symmetry along the stacking direction

rule: the greek letter must be converted to the remaining greek letter, i. e., the one not corresponding to the layer of the inversion center and not being the letter of the original sequence. This remaining letter must then exist at the equal distance away from the center of symmetry along the stacking direction

… between two c-type layers?

the same rules apply as for the octahedron between two h-type layers

Which conditions must be met for the stacking sequence to obtain inversion symmetry on a AX_{12} cuboctahedron?

rule: the same letter must exist at the equal distance away from the center of symmetry

rule: the same greek letter must exist at the equal distance away from the center of symmetry

rule: the greek letter must be converted to the remaining greek letter, i. e., the one not corresponding to the layer of the inversion center and not being the letter of the original sequence. This remaining letter must then exist at the equal distance away from the center of symmetry along the stacking direction

rule: the roman letter must be converted to the remaining roman letter, i. e., the one not corresponding to the layer of the inversion center and not being the letter of the original sequence. This remaining letter must then exist at the equal distance away from the center of symmetry along the stacking direction

Which conditions must be met for the stacking sequence to obtain a mirror plane on a AX_{12} anti-cuboctahedron perpendicular to the direction of stacking?

general rule: the same greek or roman letter must exist at the equal distance away from the center of symmetry

Figure 12. Conditions of the stacking sequence which must be met to maintain highest possible symmetry on A-site and B-site cations.

We note that the A/B/C/α/β/γ notation is not convenient to inspect this symmetry. From inspecting the Jagodzinski notation, we can immediately derive a much simpler rule: The inversion symmetry (A cation in c-type layer or B cation) or mirroring symmetry perpendicular to the mirror plane (A cation in h-type layer) is pertained whenever the Jagodzinski notation can be mirrored / inverted at one letter or between two letters – since the stacking sequence in Jagodzinski notation is one-dimensional, both operations are in principle identical. One can now summarize and simplify the rules and considerations derived so far within four simple statements (and one exception), by inspecting if the stacking sequence in the Jagodzinski notation can be mirrored/inverted at some point (which is not to be confused with mirror/inversion symmetry within the crystal structure):

- The A-site cations within an h-type layer possess local symmetry of -6 *m* 2, if the whole stacking sequence given in the Jagodzinski notation can be mirrored at this layer.

  Example: …chchhccchchhhchccchhchc…

- The A-site cations within a c-type layer possess a local symmetry of -3 2/*m*, if the whole stacking sequence given in the Jagodzinski notation can be mirrored at this layer.

  Example: …chchhccchchChchccchhchc…

- The B-site cations between two c-type layers or between two h-type layers possess a local symmetry of -3 2/*m*, if the whole stacking sequence given in the Jagodzinski notation can be mirrored between these two layers.

  Examples: …cchchchc Chchchcc… or …cchchchh hhchchcc…

- For any other case, the maximum symmetry of the A-site cation or the B-site cation is 3 *m*.

  Examples: …chCch… or …chhch… or …chc Cch… or …chh hch…

- The only exemption to these rules is the simple case of only c-type layers (…ccc…). This results in a higher symmetry on both, the A-site and the B-site cations of 4/*m* -3 2/*m.*

We can now return to our previous statement and summary: The Jagodzinski notation is one-dimensional and every aristotype perovskite which contains at least one h-type layer can be described via a unique sequence of h and c with a length of n units of h and/or c symbols. What symmetries are allowed for a sequence of two letters? To understand this, we simply need to imagine this unique sequence of two letters as one of two different type of arrows as shown in Figure 13. We conclude: along a single unique stacking sequence, we can either find two symmetries (inversion and/or mirroring) for the double arrow (in the middle of the arrow or between the double arrows, see Figure 13a). Alternatively, one can find no symmetry of the unique stacking sequence, as indicated by the singe arrow, see Figure 13b.

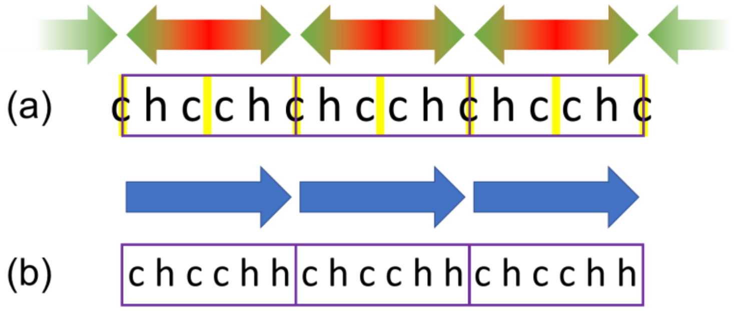

Figure 13. Scheme on how symmetry operations can be distributed within a unique Jagodzinski stacking sequence. Only two scenarios are possible: (a) The stacking sequence, indicated by a double arrow, has mirroring / inversion symmetry in the middle of the arrow and between the arrows in a pattern of repetition of the unique sequence. (b) The Jagodzinski notation cannot be mirrored / inverted and is thus represented by a single arrow.

2.2 From local symmetry to space group symmetry

The local symmetry considerations derived above are sufficient to describe the size, the local site symmetry as well as the overall space group symmetry, if the stacking sequence is given. To move over from a local site symmetry to space group symmetry, one must include the translational symmetry included in each lattice. This translational symmetry is not only given by the size of the unit cell but can also be included in the centering of the space group (in our case: the *R*-centering). Further, translation can be combined with symmetry operations, resulting in screw axes (e.g., the 6_3 screw axis) or glide planes (e. g., the *c* glide plane).

First, we want to derive the size of the unit cell required to describe the stacking sequence. To do so, we write down the sequence in both, ABC notation, and Jagodzinski notation. By this, we can derive the number of layers that must be given after which both notations repeat. This is exemplified in Figure 14 for the three sequences ch, cch, and chcch, which show that inspecting the stacking sequence in the Jagodzinski notation is not sufficient to determine the length of the unit cell along the stacking direction. We conclude that the stacking sequence in A/B/C/α/β/γ is required to describe the length of the unit cell and number of AX_3 layers found within a unit cell correctly. The number of layers in A/B/C/α/β/γ notation required to obtain repetition can thus be used to label perovskite material (e.g., 3C, 6H, 15R, …). So far it does not tell us about the letter that follows after, nor we could derive the space group from this symbol.

	repeats after … units																		
Jagodzinski notation	2	h	c	h	c	h	c												c-axis length ==> 2 x layer thickness
stacking sequence	4	B	A	B	A	C	A												
Jagodzinski notation	3	h	c	c	h	c	c	h	c										c-axis length ==> 6 x layer thickness
stacking sequence	6	C	A	B	C	B	A	C	A										
Jagodzinski notation	5	h	c	h	c	c	h	c	h	c	c	h	c	h	c	c	h	c	c-axis length ==> 15 x layer thickness
stacking sequence	15	C	A	B	A	C	B	C	A	C	B	A	B	C	B	A	C	A	

Figure 14. Examples on how to derive the length of the unit cell axis from the stacking sequence. The axis of stacking will become the crystallographic c-axis.

For the following discussion, we can neglect the positions of the B-site cations and their Greek letters and focus on the main stacking sequence A/B/C entirely. First, we determine a suitable two-dimensional cell size within the close packed AX_3 layers, which we place within the *ab*-plane. By this, the direction of stacking perpendicular to the plane becomes the *c*-axis. It is simple to derive the positioning of atoms within differently oriented AX_3 or B layers within it. To get these positions of cations and anions within the cell, we remind on our definition from before: the layers of composition AX_3 are described as close packed spheres with $r(A) = r(X)$, and the B cations have a radius to fit exactly into an octahedron formed by an X cation, i.e., $r(B) = (2^{0.5}-1)\ r(X)$. The stacking along the c-direction is done in such a way to maximize space filling efficiency. From these conditions, we can derive the shape and the size of the unit cell perpendicular to the stacking direction as shown in Figure 15. Due to this maximum density approach, this two-dimensional cell contains only one AX_3 unit or one B atom. For simplicity, we put either the A or the B cation on the origin of the cell (within the International Tables of Crystallography, the highest symmetric sites are usually placed at the origin). The cell size can be calculated according to $a = b = 4\ r(X)$ with an angle $\gamma = 120°$ between the *a*-axis and the *b*-axis.

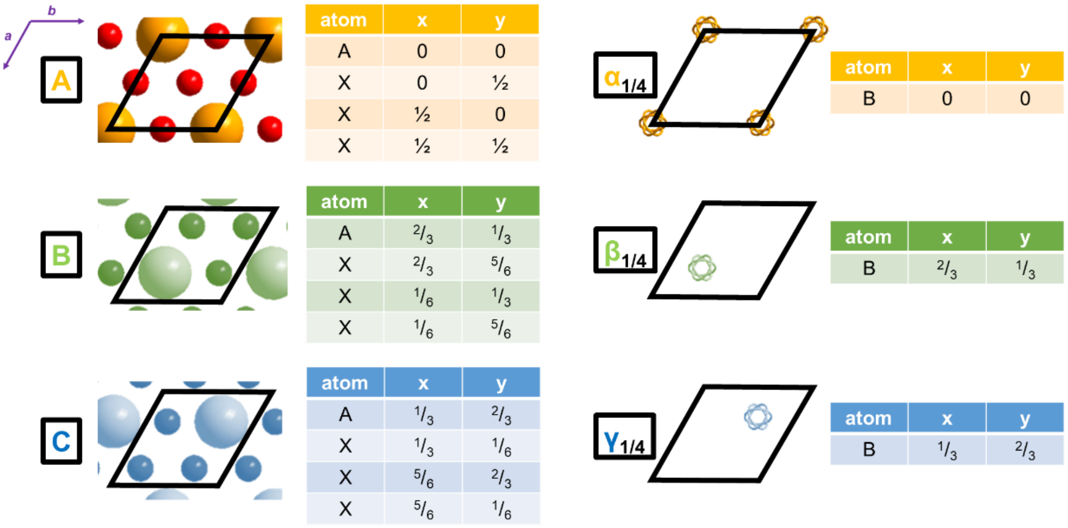

atom	x	y
A	0	0
X	0	½
X	½	0
X	½	½

atom	x	y
A	$^{2}/_{3}$	$^{1}/_{3}$
X	$^{2}/_{3}$	$^{5}/_{6}$
X	$^{1}/_{6}$	$^{1}/_{3}$
X	$^{1}/_{6}$	$^{5}/_{6}$

atom	x	y
A	$^{1}/_{3}$	$^{2}/_{3}$
X	$^{1}/_{3}$	$^{1}/_{6}$
X	$^{5}/_{6}$	$^{2}/_{3}$
X	$^{5}/_{6}$	$^{1}/_{6}$

atom	x	y
B	0	0

atom	x	y
B	$^{2}/_{3}$	$^{1}/_{3}$

atom	x	y
B	$^{1}/_{3}$	$^{2}/_{3}$

Figure 15. Derivation of idealized positions of atoms under the condition that AX_3 form close packed layers of spheres with r(A) = r(X), and the B cation fits exactly into the octahedral site formed by 6 X anions with $r(B) = (2^{0.5}-1)\ r(X)$.

We easily note from Figure 15 that a mirroring symmetry can exist perpendicular to the [1 1 0] direction. In addition, the 3 m symmetry, which is the minimal symmetry maintained for the A-site and the B-site cations independent on the detailed stacking direction, must be present along the stacking direction running through [0 0], [1/3 2/3], and [2/3 1/3]; alternatively, -3 2/*m* or -6 2 *m* symmetry can also found at these positions, since they contain the 3 *m* symmetry as a subgroup. We can inspect the International Tables for Crystallography for space groups within the trigonal or hexagonal crystal systems, which possess these site symmetries in a suitable pattern. These space groups are *R*-3*m*, *R*3*m*, $P6_3/mmc$, $P6_3mc$, *P*-6*m*2, *P*-3*m* and *P*3*m* (see Figure S 1). It will be derived in the following which conditions must be met for a perovskite-type material with at least partial h-type stacking of AX_3 layers to crystallize in one of these space groups. We recognize that the first four space groups have additional translational symmetry (*R*-centering or 6_3 screw axes (in addition to a c-glide plane)), and we will see that these space groups are relevant, whenever the unique stacking sequence in Jagodzinski notation has to be repeated three (*R*) or two (6_3) times to obtain a repetition of the A/B/C/α/β/γ notation.

We also note from Figure 15 that we can transform the two dimensional layers between each other by adding the translational vector [+1/3 +2/3] once or twice. This translational component is of principle importance for the R-centering within the trigonal crystal system, for which we require additional translation along the stacking direction. The 3D condition for *R*-centering is that the vectors [+2/3 +1/3 +1/3] and [+1/3 +2/3 +2/3] can be added (within a cell of a = b ≠ c, α = β = 90°, γ = 120°) to find symmetry equivalent points. We can ask ourselves now what condition must be met for the stacking sequence to find an R-centering of the trigonal cell.

Since the R-centering requires translation of 1/3 along the c-direction, this condition can only be met if 3n (with n ∈ ℕ* being the length of the unique Jagodzinski notation) layers form the repetitive pattern of the stacking sequence A/B/C/α/β/γ notation. Consequently, the stacking sequence follows a permutation pattern as shown in Figure 16.

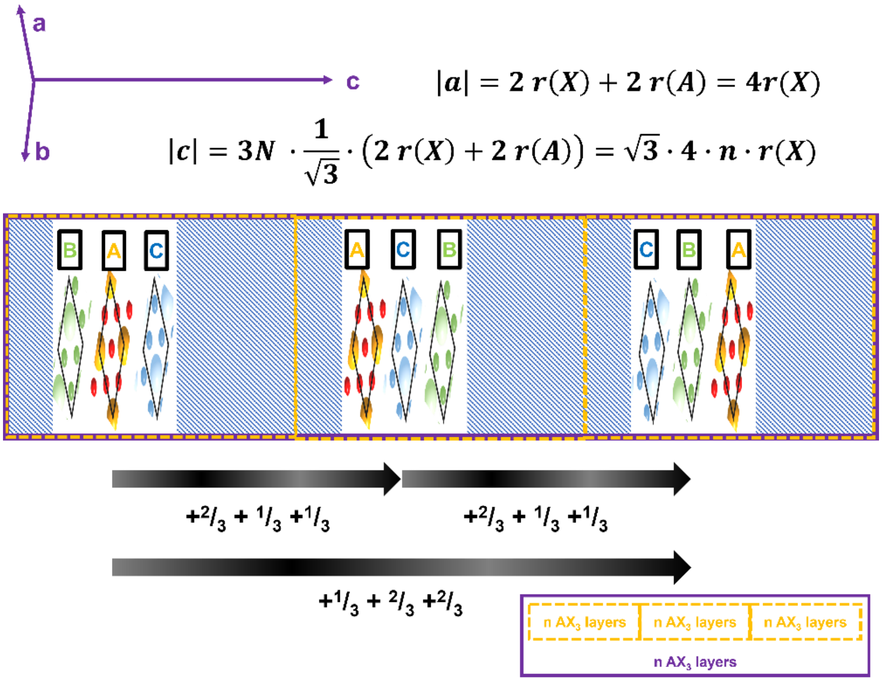

Figure 16. Permutation pattern of AX_3 layers within a unit cell containing 3N close-packed AX_3 layers to fulfill the condition of R-centering within the trigonal crystal system.

Since the R-centering can only be found in the trigonal crystal system, we can further conclude that this stacking must result in the lowering of the -6 = 3/*m* symmetry on any h-type layer to 3-fold rotational symmetry; in other words: h-type layers must be sandwiched in such a way that the mirroring symmetry will be broken. However, it is possible to maintain inversion symmetry on A-site cations in c-type layers or on the octahedrally coordinated B-site cations (see Figure 17a), e. g., as found for the $(chcch)_3$ stacking sequence which has an inversion center on both, A- and B-site cations. We also note that the h-type layers do not necessarily need to be found on a local chh surrounding, but that different numbers c_k / c_j (with k ≠ j) on both sides of h can also break the mirroring symmetry. The perovskite material corresponding to a unique stacking sequence of length n should be described as a (3n)*R*-type perovskite compound with inversion symmetry, and the resulting space group is *R*-3*m*. This symmetry is indeed found for certain perovskite-type materials, e. g., 15R-$BaFeO_2F$ [6].

For this example, we have seen that the inversion or mirroring symmetry can in principle be broken by the stacking sequence, although the local coordination from the next nearest layers (e. g. …*chc*…) would not break the corresponding symmetry per se. Therefore, we can also search for examples, for which a non-symmetric unique Jagodzinski notation must be repeated three times to describe the unit cell. This can be obtained for the sequence (*chcchccchcccch*)$_3$, which fulfills the *R*-centering condition, but does not allow inversion symmetry or mirroring symmetry perpendicular to the stacking direction on any of the A-site or B-site cations (see Figure 17b). The highest local symmetry is 3*m* for both cation types, resulting in an overall maximum space group symmetry of *R*3*m*. We note that it might require a comparably long unique Jagodzinski unit to break the inversion symmetry, and this most likely explains why this stacking and space group has not been observed experimentally so far for perovskite-type materials to the best of our knowledge.

Given that R-centering within the trigonal crystal system can result in two different space groups, we suggest indicating this with an additional superscript. For this purpose, we propose to use “*i / I*” as superscripts to indicate a center of symmetry found either on an A-site cation (i) or on a B-site cation (I) for *R*-3*m*. Alternatively, once could use the symbol “*” to indicate the absence of inversion symmetry AND a mirror plane perpendicular to the direction of stacking. Thus, the examples given in Figure 17 could be described as 15R^{iI} and 42R* perovskite-type modifications.

(a) **stacking sequence (chcch)$_3$ with N = 5**

→ 3 repetitions of Jagodzinski notation required AND maximum local site symmetry is -3*m*; resulting maximum space group symmetry: ***R*-3*m*** → **15*R*^{ii}**

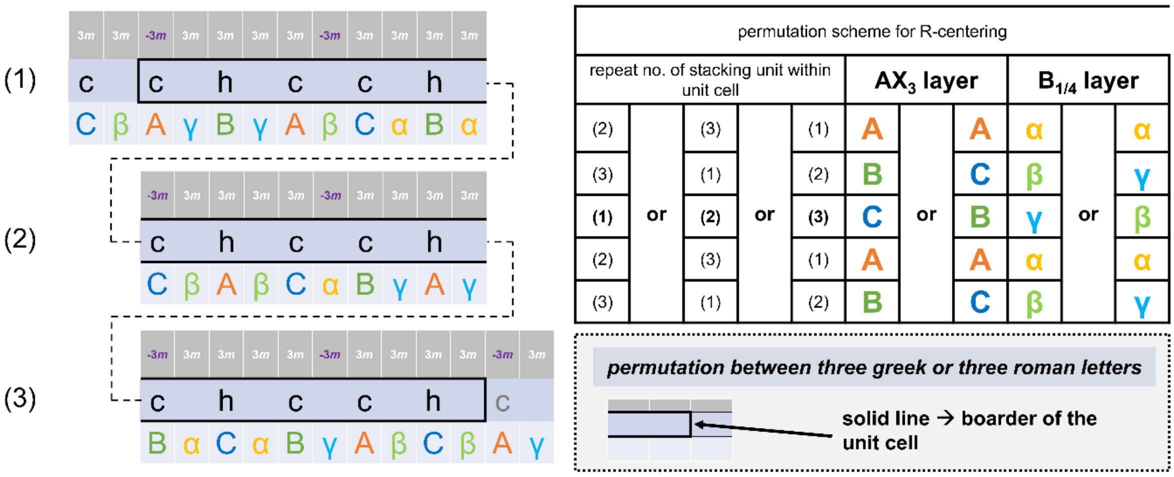

permutation scheme for R-centering										
repeat no. of stacking unit within unit cell					**AX$_3$ layer**			**B$_{1/4}$ layer**		
(2)		(3)		(1)	A		A	α		α
(3)		(1)		(2)	B		C	β		γ
(1)	**or**	**(2)**	**or**	**(3)**	C	**or**	B	γ	**or**	β
(2)		(3)		(1)	A		A	α		α
(3)		(1)		(2)	B		C	β		γ

-3*m* found on c-type layers (A, B, and C), which are in a local …cch**c**hcc… surrounding

3*m* found on c-type layers in local ….h**c**c… surrounding

3*m* found on h-type layers surrounded by different numbers of c-type layers, i.e., …hc**h**cch… breaks mirroring symmetry perpendicular to stacking direction

-3*m* found on α, β, and γ between …hc ch…

3*m* found on α, β, and γ between …h c… due to breaking of inversion symmetry

(b) **stacking sequence (chcchccchcccch)$_3$ with N = 14**

→ 3 repetitions of Jagodzinski notation required AND maximum local site symmetry is 3*m*; resulting maximum space group symmetry: ***R*3*m*** → **42R***

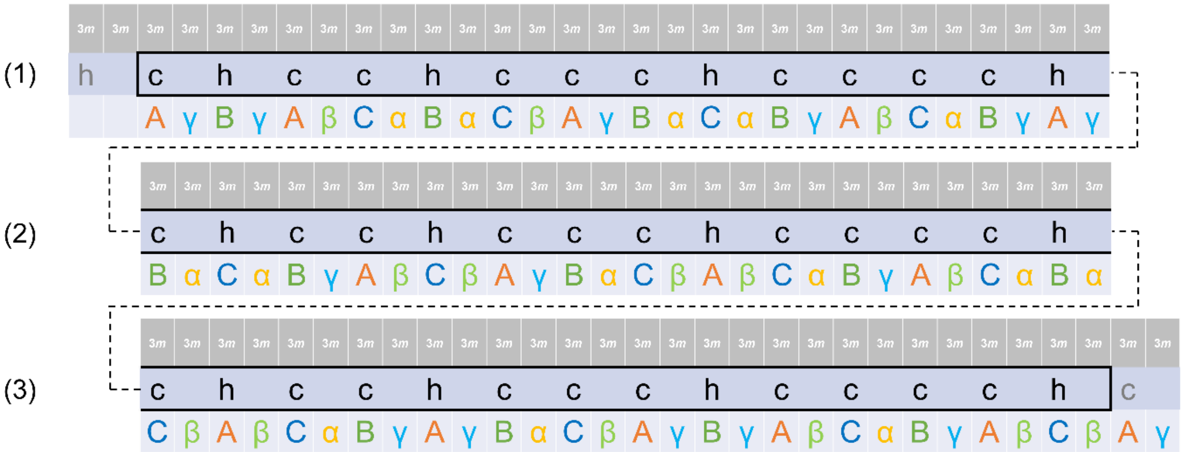

3*m* found on c-type layers in local ….h**c**c… surrounding due to breaking of inversion symmetry

3*m* found on h-type layers surrounded by different numbers of c-type layers, i.e., …c$_n$**h**c$_m$… breaks mirroring symmetry perpendicular to stacking direction since n ≠ m

3*m* found on c-type layers in surroundings such as…c$_n$**c**c$_m$… / …c$_n$h**c**hc$_m$… / …c$_n$hc$_l$**c**c$_l$hc$_m$… ; n ≠ m breaks inversion symmetry

3*m* found on α, β, and γ between …c$_n$hc$_l$ c$_l$hc$_m$… / …hc$_n$ c$_m$h… / ; n ≠ m breaks inversion symmetry

3*m* found on α, β, and γ between …h c… due to breaking of inversion symmetry

Figure 17. Deriving possible space group symmetries for R-centered perovskite materials with partial h-type AX$_3$ layers.

The R-centering is the only centered Bravais lattice for the trigonal crystal system. In the hexagonal crystal system, centering does not exist. To understand how to create additional translational symmetry in the hexagonal crystal system, we need to understand how translation can be combined with 6-fold rotational symmetry for the highly symmetric polyhedra of perovskite type compositions. Neither the octahedron, nor the cuboctahedron nor the anti-cuboctahedron contain a proper 6-fold rotational axis. If we apply a hypothetical 6-fold rotation along to the stacking direction to either of these polyhedra, we observe that the central layer (i.e., either the layer containing the respective A-site or B-site cation) maintains its original orientation, while the layers on top or on bottom switch their respective orientation (i.e., B (green) seems to transform to C (blue) and vice versa, see Figure 18). Thus, it is possible to combine 6-fold rotation with translational symmetry within a 6_3 screw axis, which requires that the unique stacking sequence in the Jagodzinski notation with length n repeats twice within the length of the unit cell. The corresponding perovskite materials should be described as (2n)H perovskite materials.

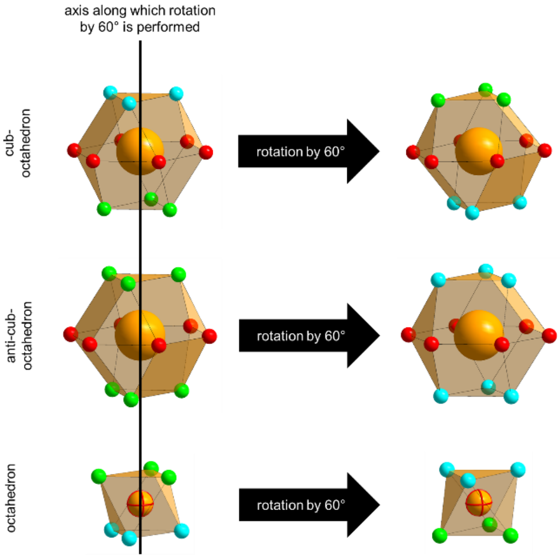

Figure 18. Application of a hypothetical 6-fold rotation axis along the stacking direction to the different polyhedra which can be found for A-site or B-site cations.

Further, if we write out the stacking sequence fully, it must contain

- one unique greek letter representing the layer containing the B-site cation which is found again after translating half distance along the stacking direction (see Figure 19a)
- one unique roman letter representing the AX_3 layer which is found again after translating half distance along the stacking direction (see Figure 19b)
- one unique roman letter representing the AX_3 layer and the corresponding greek letter representing the layer contain the B-site cation which are both found again after translating half distance along the stacking direction (see Figure 19c)

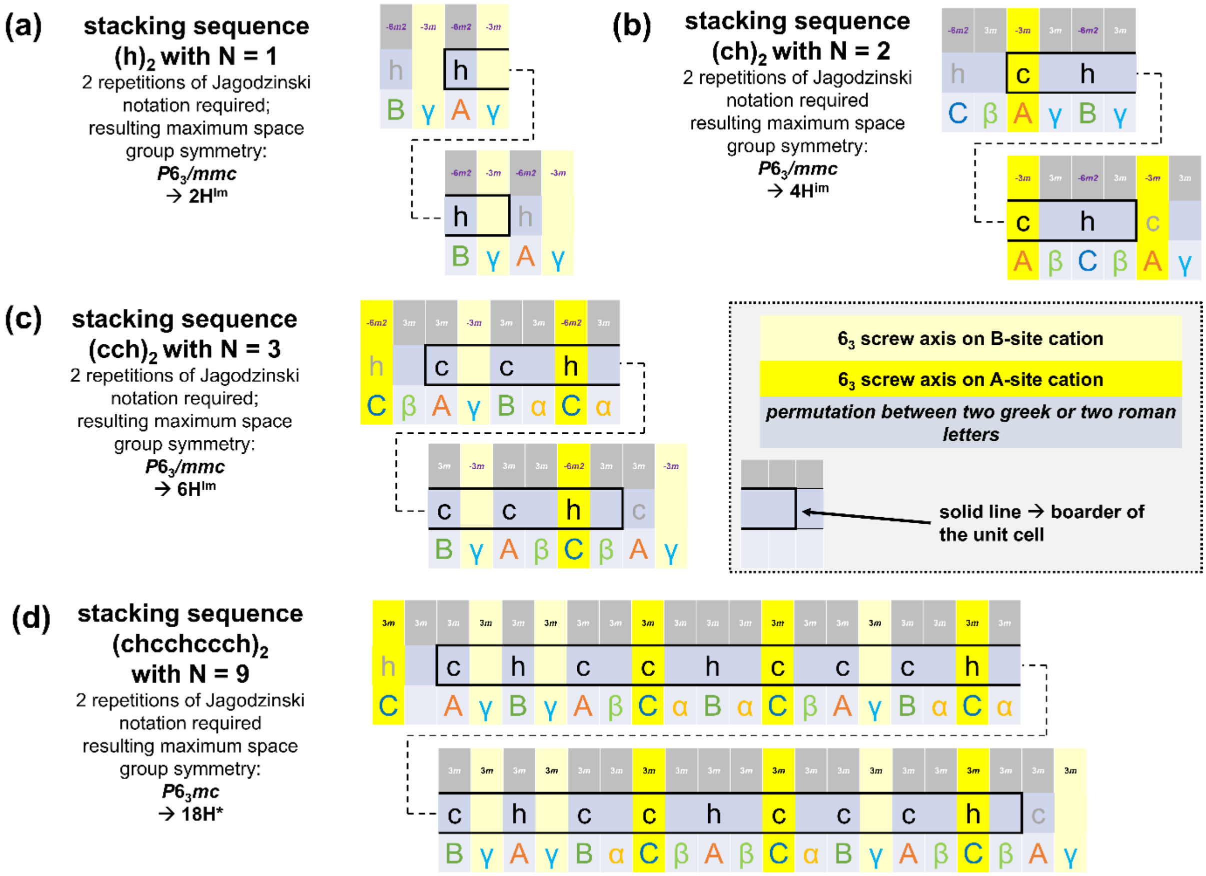

Figure 19. Conditions on the stacking sequence to obtain a 6_3 rotation axis and maintain a center of symmetry. The possible space group symmetries are $P6_3/mmc$ and $P6_3mc$. The same rules apply for assigning local symmetries 3m, -3m, -6m2 as shown in Figure 17.

Without further proof, it is found that the 6_3 screw axis also results in a c-glide plane perpendicular to the [2 1 0] direction. If the unique stacking sequence in Jagodzinski notation contains one A-site cation on an h-type layer with high symmetry -6 *m* 2, and one A-site cation in a c-type layer or a B-site cation with -3 *m* symmetry between two h-type layers or a B-site cation with -3 *m* symmetry between two h-type layers, the highest possible symmetry of these sequences is $P6_3/mmc$ (remember: the $6_3/m$ axis contains $3/m$, and generates a mirror plane perpendicular to the 6_3 axis along the stacking direction). All these compounds will contain one A- or B-cation with -3*m* symmetry and one A-cation with -6 *m* 2 symmetry within their unique Jagodzinski notation.

As shown in Figure 19d, obtaining the condition for a 6_3 axis is decoupled from having local -3 *m* or -6 *m* 2 site symmetries, and one can also obtain stacking sequences which possess a 6_3 rotation axis, but do not contain high symmetry A- or B-cations. These stacking sequences will result in a space group of $P6_3mc$, see Figure 19d. Their unique Jagodzinski sequence is repeated twice to obtain the unit cell in A/B/C/α/β/γ notation. In that case, the perovskite compound would become polar, and these aristotype stacking sequences have not been observed for perovskite-type materials so far (see also later in this article).

Since the presence of a 6_3 screw axis within the hexagonal crystal system can result in two different hexagonal space groups, we again would recommend that this could be indicated by an additional superscript. For this we again suggest to use “i/I” to indicate a center of symmetry found for $P6_3/mmc$ on A-site or B-site cations in addition to “m” to indicate the presence of a mirror plane perpendicular to the stacking direction (which will always be on the A-site cation in h-type layers) or to use “*” to indicate the absence of inversion symmetry AND a mirror plane perpendicular to the direction of stacking as found for $P6_3mc$. Thus, the examples given in Figure 19 could be described as $2H^{Im}$, $4H^{im}$, $6H^{Im}$ and 18H* perovskite-type modifications.

The R-centering and the 6_3 rotational axis are the only centering operation or symmetry elements with translational symmetry which can exist for aristotype structures of perovskite materials with h-type layers. If the unique Jagodzinski notation does not have to be repeated to obtain the size of the unit cell in the A/B/C/α/β/γ notation ($n = 1$), there are three further possibilities for symmetries which can be found. They have in common that they can be determined from the maximum symmetry found for the A- or B-site cation in combination with P-centering.

- If two A-site cations are located on h-type layers and possess a local symmetry of $-6m2$ within the unique Jagodzinski sequence, the resulting space group symmetry will be $P\text{-}6m2$ (see Figure 20a)
- If two A-site cations on c-type layers and/or B-type cations possess a local symmetry of $-3m$, the resulting space group symmetry will be $P\text{-}3m$ (see Figure 20b)
- If the highest symmetry for any of the A- and B-site cations is 3m, the resulting space group symmetry will be $P3m$ (see Figure 20c)

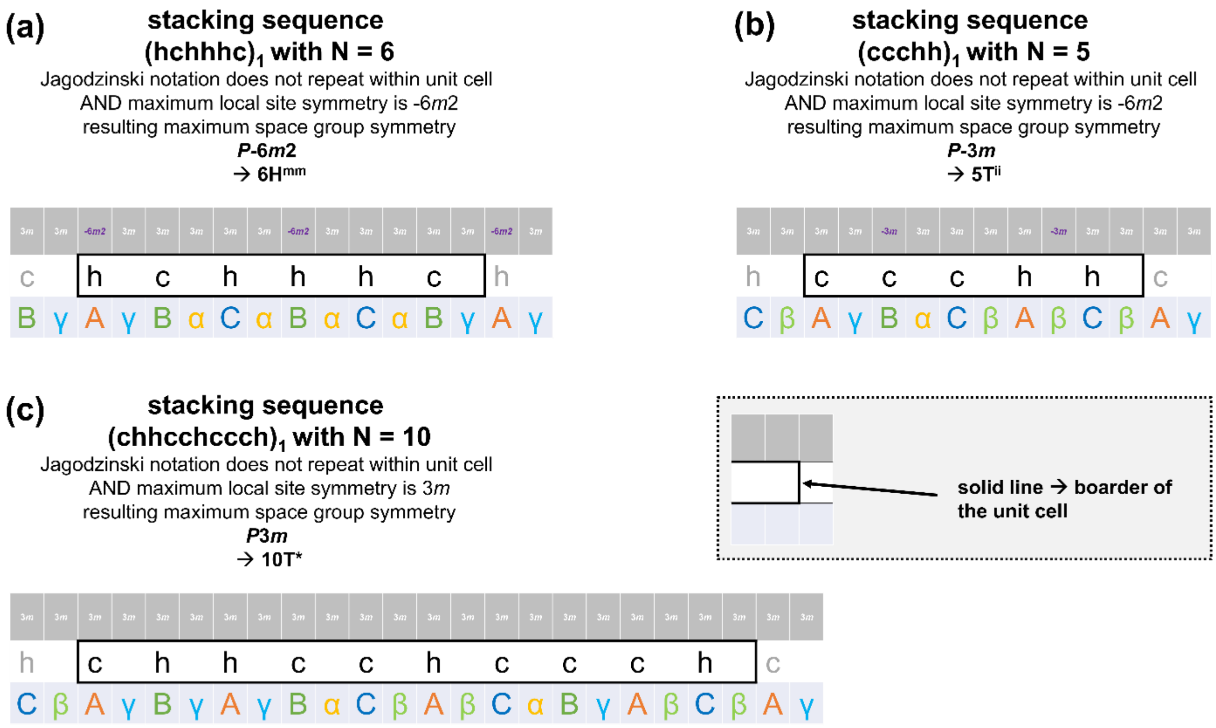

Figure 20. Stacking sequences with Jagodzinski notations which do not repeat within a single unit cell. Resulting space groups are P-6m2, P-3m, and P3m. The same rules apply for assigning local symmetries 3m, -3m, -6m2 as shown in Figure 17.

We note that *P*-3*m* and *P*3*m* are space groups within the trigonal primitive crystal system. We also note that P-6*m*2 is another possible hexagonal symmetry. Thus, the periodicity of a unique Jagodzinski sequence with length of n after one repetition (1n) results in trigonal or hexagonal perovskite modifications. Since *P*-6*m*2 contains mirroring symmetry perpendicular to the direction of stacking, but does not contain a center of symmetry, the stacking sequence (*hchhhc*)$_1$ shown in Figure 20a could be described as 6H^{mm} perovskite-type compound. This would make the material clearly distinguishable from the 6H^{lm} perovskite-type material with stacking sequence (*cch*)$_2$ described in Figure 19c, and could allow easy assignment of the maximum space group symmetry from the commonly used notification. Further, we also think that the notation should be extended to the trigonal primitive crystal system by using the letter T and indicating if they possess ('*i*' or 'l') or do not possess ('*') a center of symmetry. Therefore, the perovskite materials depicted in Figure 20b,c would be denoted as 5T^{ii} and 5T* materials. With the notation proposed here, it becomes feasible to assign the maximum symmetry of the material based on the stacking notation and relate the material to an aristotype easily.

2.3 Reduction of the aristotype symmetry in perovskites with h-type AX$_3$ layers

Occasionally, also orthorhombic symmetries can be found for "hexagonal" perovskite materials, e.g., for 10H^{lm} compounds (mirror plane and inversion perpendicular to lattice parameter *c*). However, in this case, the orthorhombic crystal system is not related to the stacking of the material but originates from the presence of vacancies and their ordering for example in $Ba_5In_{0.93}Mn_4O_{14.4}$ [27]; in absence of the vacancies, the material could have a higher symmetry. We thus note: **Any orthorhombic, monoclinic, or triclinic symmetry can never be the aristotype symmetry corresponding to a unique Jagodzinski sequence of perovskites with h-type layers**. These symmetry changes are related to what has been found for structures deriving from the cubic aristotype, and can originate from anion ordering, distortions due to size mismatches, electronic effects, etc. [17]. We can also formulate a trivial statement: Cubic and tetragonal crystal systems cannot be obtained for perovskite materials with h-type AX_3 layers.

A couple of perovskite materials with h-type layers and polar space group symmetry have been reported. Mainly, the symmetry lowering originates from a combination of cation ordering of mixed occupied B-site cations in combination with electronic effects, e.g., $Ba_{14}Mn_{1.75}Ta_{10.5}O_{42}$ [28]. For none of these compounds the polar symmetry originates from the aristotype symmetry of the corresponding stacking sequence. In addition, there was a recent example of a polar hexagonal perovskite $BaWON_2$ $(cch)_2$ and space group $P6_3mc$ [29]. Similarly, the polar space group does not result from the stacking, but from electronic effects of the tungsten atoms, causing individual off-center shifts. Hence, the aristotype symmetry of AX_3 layers in this material would formally be described as $6H^{im}$, and the symmetry lowering results from a *translationengleiche* symmetry transition (*t*2) from $P6_3/mmc$ to $P6_3mc$. Thus, we would also like to emphasize that group-subgroup relations [30] between the seven possible aristotype space group symmetries of perovskites with h-type layers exist in principle (as shown in Figure 21). Thus, we point out that symmetries lower than the aristotype symmetries could be formed if further reasons (electronic effects, ion sizes, etc.) for symmetry breaking exist. The reduced subgroup symmetries should not be confused as the aristotype symmetry of the material, but are clearly hettotype structures; however, so far there are onlyfew examples with symmetry reductions of the aristotype symmetry.

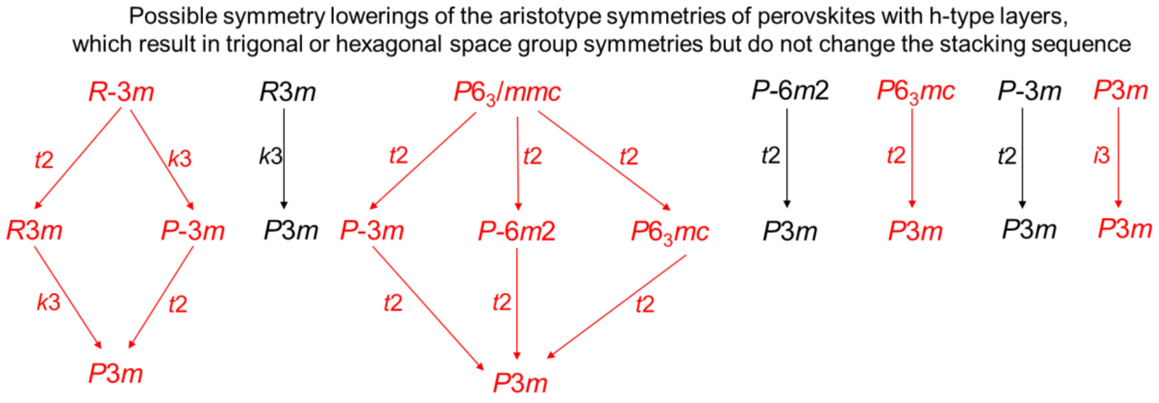

Figure 21. Possible symmetry lowerings of the aristotype symmetries of perovskites with h-type layers, which result in trigonal or hexagonal space group symmetries but do not change the stacking sequence.

2.4 PerovGen – A computer program for analyzing Jagodzinski stacking sequences of perovskites with mixed *h*-type and *c*-type layers

The strategy for achieving the highest symmetry possible by only considering the stacking sequence along the lattice parameter *c* is effective, provided there are no other chemical or structural effects causing a symmetry reduction. We have developed a program called *PerovGen* (details on the programming are provided in the supplementary material), which can determine the highest possible symmetry of a perovskite material ABX_3 of any unique stacking sequence $c_n h_m c_l h_k$… ($n,m \in \mathbb{N}^*$; $k,l,etc. \in \mathbb{N}_0$). The program is freely available from [31]. It analyses perovskite stacking sequences, determines the number of repetitions of Jagodzinski notations to describe the unit cell in the A/B/C/α/β/γ notation and determines the symmetry positions of the Jagodzinski notation. This procedure is related to the flow chart shown in Figure 22, from which the space group can be assigned. Additionally, it generates a CIF file of the specified Jagodzinski sequence by using the atomic positions as shown in Figure 15, determining a necessary shift of origin as required from the position of the special sites according to the International Tables of Crystallography A (also see summary in Table S 1).

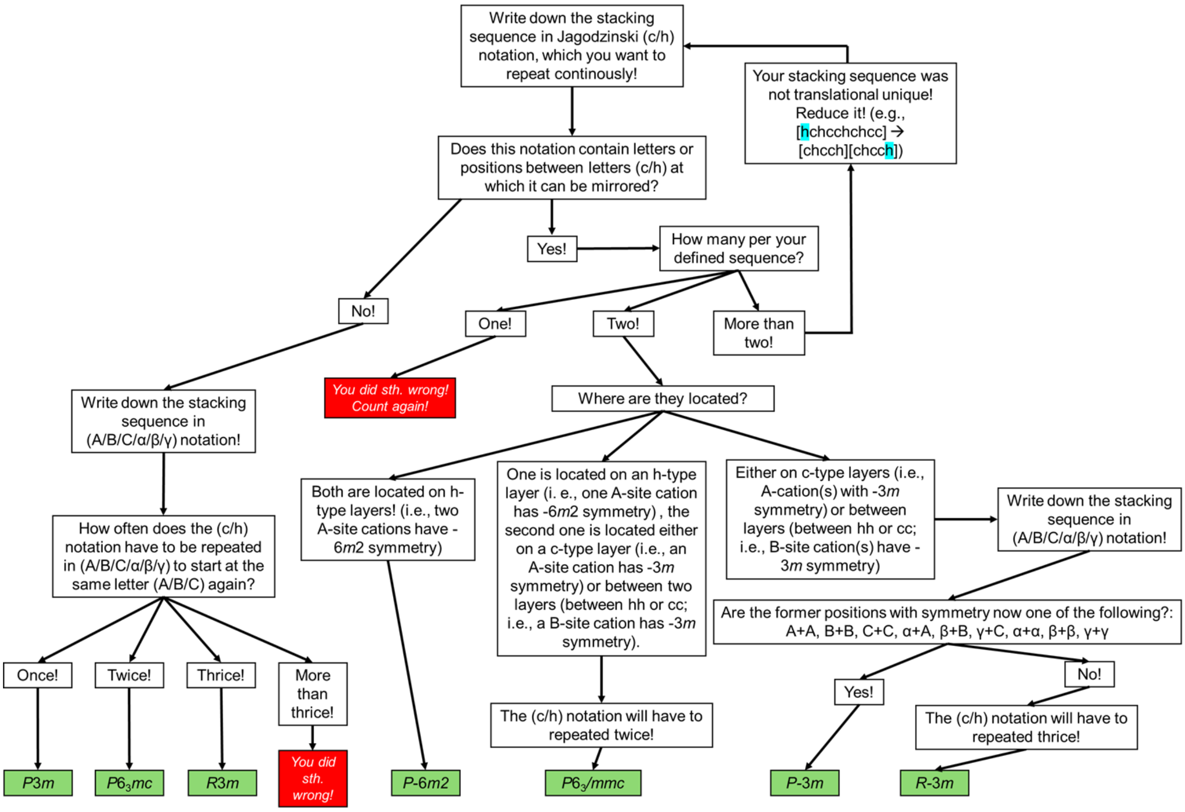

Figure 22. Flow chart which can be used to determine the symmetry of a Jagodzinski notation describing perovskite type materials with at least one h-type layer. The red boxes will help the reader to identify if a mistake was made, and or not integrated within PerovGen [31].

2.5 Applying PerovGen

We can now use the program PerovGen or the flow chart from Figure 22 to analyze, which unique stacking sequences in the Jagodzinski notation are possible up to a length of 8 *c*/*h* symbols. These possibilities are listed in Table 1 giving reference to examples of materials which are already reported in literature from a search of the ICSD database [32]. We find that for lengths smaller or equal than five *c*/*h* symbols, only centrosymmetric aristotype symmetries can be obtained (i. e., *Pm*-3*m*, *R*-3*m, P*-3*m* or $P6_3/mmc$) as depicted in Table 1. Starting from six *c*/*h* units within the unique Jagodzinski pattern, the polar space group $P6_3mc$ becomes possible for the sequence chcchh, and the non-centrosymmetric space group *P*-6*m*2 can be found for chchhh. The longer the sequence, the more often we can find the polar space groups, and this lack of periodicity might explain why such polarity originating from stacking only has not been found yet. Also, the number of possible unique Jagodzinski sequences also increases with the number of n. An overview on the distribution of space group symmetries on the length of the Jagodzinski notation is shown in Figure 23.

*Table 1. Overview of possible unique stacking sequences in Jagodzinski notation (unJag) with a length of upto n = 8 c/h symbols and resulting space group symmetry including modified notation (modNot) for perovskite-type materials with h-type layers. symJag = Symmetrical representation of the stacking sequence with inversion on A-cation (c), inversion on B-cation ( ), mirror plane on A-cation perpendicular to stacking direction (h); K = multiplication factor required to obtain unit cell size in A/B/C/α/β/γ notification; unJag = unique Jagodzinski notation; symCat = Symmetry found on the A-/B-cations with inversion on A-cation (i) in c-type layer, mirror symmetry perpendicular to stacking direction on A-cation (m), and inversion symmetry on B-cation (I); maxSGS = maximum aristotype space group symmetry; * := Pm-3m is a supergroup of R-3m.*

n	**unJag**	**symJag**	**K**	**symCat**	**maxSGS**	**modNot** **n*K$^{i/I/m/*}$**	**examples**
1	*c*	$(c_{0.5}\,c_{0.5})_\infty$	3	*iI*	*Pm-3m**	$3C^{iI}$	$SrVO_3$ [33]
1	*h*	$(\,h\,)_\infty$	2	*Im*	*P6$_3$/mmc*	$2H^{Im}$	$BaNiO_3$ [34]
2	*ch*	$(c_{0.5}hc_{0.5})_\infty$	2	*im*	*P6$_3$/mmc*	$4H^{im}$	α-$SrMnO_3$ [35]
3	*cch*	$(\,chc\,)_\infty$	2	*Im*	*P6$_3$/mmc*	$4H^{Im}$	$BaFeO_3$ [36]
	hhc	$(\,hch\,)_\infty$	3	*iI*	*R-3m*	$9R^{iI}$	$BaMnO_3$ [37]
4	*ccch*	$(c_{0.5}chcc_{0.5})_\infty$	2	*im*	*P6$_3$/mmc*	$8H^{im}$	Ba_2CrTaO_6 [38]
	chhh	$(c_{0.5}hhhc_{0.5})_\infty$	2	*im*	*P6$_3$/mmc*	$8H^{im}$	$BaMnO_3$ [39]
	cchh	$(\,ch\,hc\,)_\infty$	3	*II*	*R-3m*	$12R^{II}$	$Ba_4Ti_2Mn_2O_{12}$ [17]
5	*cccch*	$(\,cchcc\,)_\infty$	2	*Im*	*P6$_3$/mmc*	$10H^{Im}$	$Sr(Mn_{0.724}Fe_{0.276}O_{2.868})$ [40]
	cchhh	$(\,chhhc\,)_\infty$	2	*Im*	*P6$_3$/mmc*	$10H^{Im}$	$Ba_5In_{0.94}Mn_4O_{14.42}$ [27]
	chchh	$(\,hchch\,)_\infty$	2	*Im*	*P6$_3$/mmc*	$10H^{Im}$	$Ba(Ir_{0.3}Co_{0.7})O_{2.828}$ [41]
	cchch	$(\,chchc\,)_\infty$	3	*iI*	*R-3m*	$15R^{iI}$	$BaFeO_2F$ [6]
	chhhh	$(\,hhchh\,)_\infty$	3	*iI*	*R-3m*	$15R^{iI}$	$BaMnO_{2.99}$ [42]
	ccchh	$(\,hccch\,)_\infty$	1	*iI*	*P-3m1*	$5T^{iI}$	$BaVO_3$ [43]
6	*ccccch*	$(c_{0.5}cchccc_{0.5})_\infty$	2	*im*	*P6$_3$/mmc*	$12H^{im}$	-
	ccchhh	$(c_{0.5}chhhcc_{0.5})_\infty$	2	*im*	*P6$_3$/mmc*	$12H^{im}$	-
	chhhhh	$(c_{0.5}hhhhhc_{0.5})_\infty$	2	*im*	*P6$_3$/mmc*	$12H^{im}$	
	chchhh	$(h_{0.5}chhhch_{0.5})_\infty$	1	*mm*	*P-6m2*	$6H^{mm}$	$Ba_6Co_6O_{16}F$ [44]
	cchhch		2	*	*P6$_3$mc*	12H*	-
	cchchh		2	*	*P6$_3$mc*	12H*	-
	ccchch	$(c_{0.5}chchcc_{0.5})_\infty$	3	*ii*	*R-3m*	$18R^{ii}$	-
	cccchh	$(\,hcc\,cch\,)_\infty$	3	*II*	*R-3m*	$18R^{II}$	-
	cchhhh	$(\,hhc\,chh\,)_\infty$	3	*II*	*R-3m*	$18R^{II}$	-
7	*cccccch*	$(\,ccchccc\,)_\infty$	2	*Im*	*P6$_3$/mmc*	$14H^{Im}$	$Ba_{14}Mn_{1.75}Ta_{10.5}O_{42}$ [28]
	ccccchhh	$(\,cchhhcc\,)_\infty$	2	*Im*	*P6$_3$/mmc*	$14H^{Im}$	-
	cchhhhh	$(\,chhhhhc\,)_\infty$	2	*Im*	*P6$_3$/mmc*	$14H^{Im}$	-
	cchcchh	$(h_{0.5}\,cchcch\,h_{0.5})_\infty$	2	*Im*	*P6$_3$/mmc*	$14H^{Im}$	-
	cchchch	$(\,chchchc\,)_\infty$	2	*Im*	*P6$_3$/mmc*	$14H^{Im}$	-
	chchhhh	$(\,hhchchh\,)_\infty$	2	*Im*	*P6$_3$/mmc*	$14H^{Im}$	-
	chhchhh	$(\,hchhhch\,)_\infty$	2	*Im*	*P6$_3$/mmc*	$14H^{Im}$	-
	ccchhch		2	*	*P6$_3$mc*	14H*	-
	ccchchh		2	*	*P6$_3$mc*	14H*	-
	cccccchh	$(\,hcccccch\,)_\infty$	3	*iI*	*R-3m*	$21R^{iI}$	-
	ccchcch	$(c_{0.5}chc\,chcc_{0.5})_\infty$	3	*iI*	*R-3m*	$21R^{iI}$	-
	chhhhhh	$(c_{0.5}hhh\,hhhc_{0.5})_\infty$	3	*iI*	*R-3m*	$21R^{iI}$	$BaMnO_{2.928}$ [45]

	chchchh	(*hchchch*)$_\infty$	3	*il*	*R*-3*m*	21R^{il}	-
	cccchch	(*cchchcc*)$_\infty$	1	*il*	*P*-3*m*1	7T^{il}	-
	ccchhhh	(*hhccchh*)$_\infty$	1	*il*	*P*-3*m*1	7T^{il}	-
	cchhchh	(*chhchhc*)$_\infty$	1	*il*	*P*-3*m*1	7T^{il}	-
	cchchhh		3	*	*R*3*m*	21R*	-
	cchhhch		3	*	*R*3*m*	21R*	-
8	*cccccccch*	$(c_{0.5}ccchcccc_{0.5})_\infty$	2	*im*	*P*6$_3$/*mmc*	16H^{im}	-
	cccccchhh	$(c_{0.5}cchhhccc_{0.5})_\infty$	2	*im*	*P*6$_3$/*mmc*	16H^{im}	-
	ccchhhhh	$(c_{0.5c}hhhhhcc_{0.5})_\infty$	2	*im*	*P*6$_3$/*mmc*	16H^{im}	-
	ccchchch	$(c_{0.5}chchchcc_{0.5})_\infty$	2	*im*	*P*6$_3$/*mmc*	16H^{im}	-
	cchchcch	$(c_{0.5}hcchcchc_{0.5})$	2	*im*	*P*6$_3$/*mmc*	16H^{im}	-
	chhhhhhh	$(c_{0.5}hhhhhhhc_{0.5})_\infty$	2	*im*	*P*6$_3$/*mmc*	16H^{im}	-
	chchchhh	$(c_{0.5}hchhhchc_{0.5})_\infty$	2	*im*	*P*6$_3$/*mmc*	16H^{im}	-
	chhchchh	$(c_{0.5}hhchchhc_{0.5})$	2	*im*	*P*6$_3$/*mmc*	16H^{im}	-
	cchhhcch	$(h_{0.5}cchhhcch_{0.5})_\infty$	1	*mm*	*P*-6*m*2	8H^{mm}	-
	chchhhhh	$(h_{0.5}hhchchhh_{0.5})_\infty$	1	*mm*	*P*-6*m*2	8H^{mm}	-
	ccccchchh		2	*	*P*6$_3$*mc*	16H*	-
	ccccchhch		2	*	*P*6$_3$*mc*	16H*	-
	ccchcchh		2	*	*P*6$_3$*mc*	14H*	-
	ccchhcch		2	*	*P*6$_3$*mc*	16H*	-
	cchhchhh		2	*	*P*6$_3$*mc*	16H*	-
	cchhhhch		2	*	*P*6$_3$*mc*	14H*	-
	cchhhchh		2	*	*P*6$_3$*mc*	16H*	-
	cchchhhh		2	*	*P*6$_3$*mc*	16H*	-
	ccccchch	$(c_{0.5}cchchccc_{0.5})_\infty$	3	*ii*	*R*-3*m*	24R^{ii}	-
	ccchhchh	$(c_{0.5}chhchhcc_{0.5})_\infty$	3	*ii*	*R*-3*m*	24R^{ii}	-
	ccccchcch	(*chcc cchc*)$_\infty$	3	*ll*	*R*-3*m*	24R^{ll}	-
	ccccchhhh	(*cchh hhcc*)$_\infty$	3	*ll*	*R*-3*m*	24R^{ll}	-
	cchhhhhh	(*chhh hhhc*)$_\infty$	3	*ll*	*R*-3*m*	24R^{ll}	-
	chhchhhh	(*hchh hhch*)$_\infty$	3	*ll*	*R*-3*m*	24R^{ll}	-
	cchchhch	(*hchc chch*)$_\infty$	1	*ii*	*P*-3*m*1	8T^{ii}	-
	cccccchh	(*hccc ccch*)$_\infty$	1	*ll*	*P*-3*m*1	8T^{ll}	-
	cchchhch	(chch hchc)$_\infty$	1	*ll*	*P*-3*m*1	8T^{ll}	-
	ccchchhh		3	*	*R*3*m*	24R*	-
	ccchhhch		3	*	*R*3*m*	24R*	-
	cchchchh		3	*	*R*3*m*	24R*	-

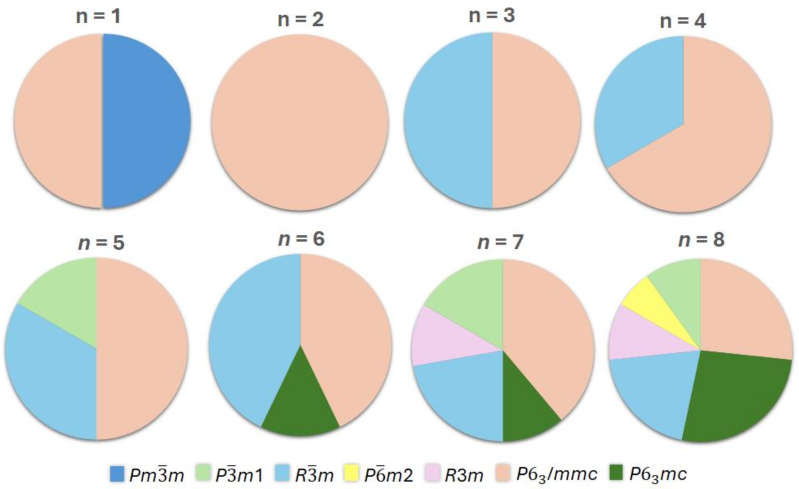

Figure 23. Distribution of space group symmetries for different lengths n of the unique Jagodzinski stacking sequence.

3 Conclusions

In the present work, we have provided a systematic guideline on how to inspect stacking sequences and derive the corresponding aristotype space group symmetry. We have shown that for perovskites with at least partial h-type stacking of AX_3 layers, every unique stacking sequence corresponds to a single aristotype structure, which will adopt one of seven possible space group symmetries.

Similar to Glazer notation, an extension of the commonly used notation to describe the size of the unit cell could be helpful in order to derive the underlying maximum space group symmetry immediately. Thus, extending the symbols by letters such as “i” and “m” will make it possible to distinguish perovskites with aristotype symmetry *P*-6*m*2 ($6H^{mm}$) from those with aristotype symmetry $P6_3/mmc$ ($6H^{lm}$) immediately. Further H^{mm} and H^{lm}/H^{im} would immediately give information on the length of the unique Jagodzinski notation: for $XH^{im}/XH^{lm}/XH^*$, the length would be $^X/_2$, for $YR^{ll}/YR^{ii}/YR^{il}/YR^{*,}$ the length would be $^Y/_3$ and for $ZH^{mm}/ZT^{ii}/ZT^*$ the length would be $^Z/_1$. However, the longer the unique stacking sequence becomes, it is possible that two different aristotype materials will still be assigned the same notation (e.g., $16H^{im}$ for *chcchcchc* and *chchhhch*). Thus, authors should be aware that they can only avoid ambiguity by giving the stacking sequence in Jagodzinski notation in addition. The program PerovGen [31] or the flow chart from Figure 22will help to assign this notation correctly.

Further, we have shown that similar to other layered perovskites, stacking of c- and h-type layers provides in principle a synthetic design tool [24] in order to make new perovskite materials without inversion symmetry. However, experimental ways must be explored to induce layer-by-layer growth of perovskite materials in order to create such materials in the future.

4 Acknowledgements

SLK and OC acknowledge funding by the German Research Foundation (DFG) via SFB 1548 FLAIR and thank the team of the Institute of Inorganic Chemistry at University of Stuttgart for helpful discussions.

5 Conflicts of Interest

There are no conflicts of interest to declare.

6 Supporting Information

Supporting information is provided for the trigonal space groups which fulfill necessary site symmetry conditions for aristotype symmetry of perovskites with partial h-type stacking as well as an overview of the crystallographic sites which can host the different cations in an ABX_3 perovskite scenario. Further we provide information on the program PerovGen [31]. References [31, 46] were cited in the Supporting Information.

7 References

(1) Fuks, D.; Mastrikov, Y.; Kotomin, E.; Maier, J. Ab initio thermodynamic study of $(Ba,Sr)(Co,Fe)O_3$ perovskite solid solutions for fuel cell applications. *Journal of Materials Chemistry A* **2013**, *1* (45). DOI: 10.1039/c3ta12874a.

(2) Basera, P.; Bhattacharya, S. Chalcogenide Perovskites (ABS_3; A = Ba, Ca, Sr; B = Hf, Sn): An Emerging Class of Semiconductors for Optoelectronics. *J Phys Chem Lett* **2022**, *13* (28), 6439-6446. DOI: 10.1021/acs.jpclett.2c01337.

(3)

(4) Akman, E.; Ozturk, T.; Xiang, W.; Sadegh, F.; Prochowicz, D.; Tavakoli, M. M.; Yadav, P.; Yilmaz, M.; Akin, S. The effect of B-site doping in all-inorganic $CsPbI_xBr_{3-x}$ absorbers on the performance and stability of perovskite photovoltaics. *Energy & Environmental Science* **2023**, *16* (2), 372-403. DOI: 10.1039/d2ee01070d.

(5) Litvin, A. P.; Margaryan, I. V.; Yin, W.; Zhang, X.; Zheng, W.; Rogach, A. L. B-Site Doping of Metal Halide Perovskite Nanoplatelets Influences Their Optical Properties. *Advanced Optical Materials* **2023**, *12* (8). DOI: 10.1002/adom.202301001.

(6) Clemens, O.; Berry, F. J.; Bauer, J.; Wright, A. J.; Knight, K. S.; Slater, P. R. Synthesis, structural and magnetic characterisation of the fluorinated compound $15R\text{-}BaFeO_2F$. *Journal of Solid State Chemistry* **2013**, *203*, 218-226. DOI: 10.1016/j.jssc.2013.04.031.

(7) Clemens, O.; Berry, F. J.; Wright, A. J.; Knight, K. S.; Perez-Mato, J. M.; Igartua, J. M.; Slater, P. R. A neutron diffraction study and mode analysis of compounds of the system La_{1-}

$_x$Sr$_x$FeO$_{3-x}$F$_x$ (x=1, 0.8, 0.5, 0.2) and an investigation of their magnetic properties. *Journal of Solid State Chemistry* **2013**, *206*, 158-169. DOI: 10.1016/j.jssc.2013.08.013.

(8) Clemens, O.; Groeting, M.; Witte, R.; Manuel Perez-Mato, J.; Loho, C.; Berry, F. J.; Kruk, R.; Knight, K. S.; Wright, A. J.; Hahn, H.; et al. Crystallographic and Magnetic Structure of the Perovskite-Type Compound BaFeO$_{2.5}$: Unrivaled Complexity in Oxygen Vacancy Ordering. *Inorganic Chemistry* **2014**, *53* (12), 5911-5921. DOI: 10.1021/ic402988y.

(9) Clemens, O.; Reitz, C.; Witte, R.; Kruk, R.; Smith, R. I. Anion ordering, magnetic structure and properties of the vacancy ordered perovskite Ba$_3$Fe$_3$O$_7$F. *Journal of Solid State Chemistry* **2016**, *243*, 31-37. DOI: 10.1016/j.jssc.2016.07.033.

(10) Clemens, O.; Wright, A. J.; Berry, F. J.; Smith, R. I.; Slater, P. R. Synthesis, structural and magnetic characterisation of the fully fluorinated compound 6H-BaFeO$_2$F. *Journal of Solid State Chemistry* **2013**, *198*, 262-269. DOI: 10.1016/j.jssc.2012.10.017.

(11) Yang, C.; Tian, Y.; Yang, C.; Kim, G.; Pu, J.; Chi, B. Recent Progress and Future Prospects of Anions O-site Doped Perovskite Oxides in Electrocatalysis for Various Electrochemical Systems. *Adv Sci (Weinh)* **2023**, *10* (35), e2304224. DOI: 10.1002/advs.202304224.

(12) Svarcova, S. Structural instability of cubic perovskite Ba$_x$Sr$_{1-x}$Co$_{1-y}$Fe$_y$O$_{3-\delta}$. *Solid State Ionics* **2008**, *178* (35-36), 1787-1791. DOI: 10.1016/j.ssi.2007.11.031.

(13) Sharif, R.; Khalid, A.; Ahmad, S. W.; Rehman, A.; Qutab, H. G.; Akhtar, H. H.; Mahmood, K.; Afzal, S.; Saleem, F. A comprehensive review of the current progresses and material advances in perovskite solar cells. *Nanoscale Adv* **2023**, *5* (15), 3803-3833. DOI: 10.1039/d3na00319a.

(14) Elkhouly, K.; Goldberg, I.; Zhang, X.; Annavarapu, N.; Hamdad, S.; Croes, G.; Rolin, C.; Genoe, J.; Qiu, W.; Gehlhaar, R.; et al. Electrically assisted amplified spontaneous emission in perovskite light-emitting diodes. *Nature Photonics* **2024**, *18* (2), 132-138. DOI: 10.1038/s41566-023-01341-7.

(15) Liu, A.; Zhu, H.; Bai, S.; Reo, Y.; Caironi, M.; Petrozza, A.; Dou, L.; Noh, Y.-Y. High-performance metal halide perovskite transistors. *Nature Electronics* **2023**, *6* (8), 559-571. DOI: 10.1038/s41928-023-01001-2.

(16) Hwang, J.; Rao, R. R.; Giordano, L.; Katayama, Y.; Yu, Y.; Shao-Horn, Y. Perovskites in catalysis and electrocatalysis. *Science* **2017**, *358* (6364), 751-756. DOI: 10.1126/science.aam7092.

(17) Tilley, R. J. D. *Perovskites: Structure-Property-Relationships*; Wiley, 2016.

(18) Howard, S. A.; Yau, J. K.; Anderson, H. U. Structural characteristics of Sr$_{1-x}$La$_x$TiO$_{3+\delta}$ as a function of oxygen partial pressure at 1400 °C. *Journal of Applied Physics* **1989**, *65* (4), 1492-1498. DOI: 10.1063/1.342963.

(19) Hoffmann, A. Sauerstoffsuren des vierwertigen Cerium und Thorium. *Die Naturwissenschaften* **1934**, *22* (13), 206-206. DOI: 10.1007/bf01504169.

(20) Arévalo-López, A. M.; Paul Attfield, J. High-pressure $BaCrO_3$ polytypes and the 5H–$BaCrO_{2.8}$ phase. *Journal of Solid State Chemistry* **2015**, *232*, 236-240. DOI: 10.1016/j.jssc.2015.09.029.

(21) Delattre, J. L.; Stacy, A. M.; Siegrist, T. Structure of ten-layer orthorhombic $Ba_5Fe_5O_{14}$ ($BaFeO_{2.8}$) determined from single crystal X-ray diffraction. *Journal of Solid State Chemistry* **2004**, *177* (3), 928-935. DOI: 10.1016/j.jssc.2003.09.032.

(22) Müller, U. *Symmetry Relationships between Crystal Structures: Applications of Crystallographic Group Theory in Crystal Chemistry.*; Oxford University Press, 2013.

(23) Glazer, A. The classification of tilted octahedra in perovskites. *Acta Crystallographica Section B* **1972**, *28* (11), 3384-3392. DOI: 10.1107/s0567740872007976.

(24) Zhu, T.; Cohen, T.; Gibbs, A. S.; Zhang, W.; Halasyamani, P. S.; Hayward, M. A.; Benedek, N. A. Theory and Neutrons Combine To Reveal a Family of Layered Perovskites without Inversion Symmetry. *Chemistry of Materials* **2017**. DOI: 10.1021/acs.chemmater.7b03604.

(25) Zhang, R.; Senn, M. S.; Hayward, M. A. Directed Lifting of Inversion Symmetry in Ruddlesden–Popper Oxide–Fluorides: Toward Ferroelectric and Multiferroic Behavior. *Chemistry of Materials* **2016**. DOI: 10.1021/acs.chemmater.6b03931.

(26) Lufaso, M. W.; Barnes, P. W.; Woodward, P. M. Structure prediction of ordered and disordered multiple octahedral cation perovskites using SPuDS. *Acta Crystallographica Section B Structural Science* **2006**, *62* (3), 397-410. DOI: 10.1107/s010876810600262x.

(27) Yin, C.; Li, G.; Jin, T.; You, L.; Tao, J.; Richardson, J. W.; Loong, C.-K.; Sun, J.; Liao, F.; Lin, J. Synthesis, Structure, and Characterization of the Hexagonal Provskite $Ba_5In_{0.93}Mn_4O_{14.40}$. *Chemistry of Materials* **2008**, *20* (6), 2110-2116. DOI: 10.1021/cm7025152.

(28) Tao, F.; Genevois, C.; Lu, F.; Kuang, X.; Porcher, F.; Li, L.; Yang, T.; Li, W.; Zhou, D.; Allix, M. First 14-Layer Twinned Hexagonal Perovskite $Ba_{14}Mn_{1.75}Ta_{10.5}O_{42}$: Atomic-Scale Imaging of Cation Ordering. *Chemistry of Materials* **2016**, *28* (13), 4686-4696. DOI: 10.1021/acs.chemmater.6b01566.

(29) Oro-Sole, J.; Fina, I.; Frontera, C.; Gazquez, J.; Ritter, C.; Cunquero, M.; Loza-Alvarez, P.; Conejeros, S.; Alemany, P.; Canadell, E.; et al. Engineering Polar Oxynitrides: Hexagonal Perovskite $BaWON_2$. *Angew Chem Int Ed Engl* **2020**, *59* (42), 18395-18399. DOI: 10.1002/anie.202006519.

(30) Bärnighausen, H. Group-Subgroup Relations Between Space Groups: A Useful Tool in Crystal Chemistry. *Match* **1980**, *9*, 139-175.

(31) Haefner, M. mhaefner-chem/PerovGen: PerovGen - v1.0.0 (v1.0.0). *Zenodo* **2024**. DOI: 10.5281/zenodo.12165868.

(32) Belsky, A.; Hellenbrandt, M.; Karen, V. L.; Luksch, P. New developments in the Inorganic Crystal Structure Database (ICSD): accessibility in support of materials research and design. *Acta Crystallographica Section B* **2002**, *B58* (3), 364-369. DOI: 10.1107/s0108768102006948.

(33) García-Jaca, J.; Mesa, J. L.; Insausti, M.; Larramendi, J. I. R.; Arriortua, M. I.; Rojo, T. Synthesis, crystal structure, stoichiometry and magnetic properties of $(Ca_{1-x}Sr_x)VO_3$. *Materials Research Bulletin* **1999**, *34* (2), 289-301. DOI: 10.1016/s0025-5408(99)00002-1.

(34) Jin, L.; Wang, H.; Xu, X.; Ni, D.; Yang, C.; Ku, Y.-C.; Liu, C.-E.; Kuo, C.-Y.; Chang, C.-F.; Sereika, R.; et al. Hidden Hydroxides in KOH-Grown $BaNiO_3$ Crystals: A Potential Link to Their Catalytic Behavior. *Chemistry of Materials* **2023**, *35* (21), 9434-9443. DOI: 10.1021/acs.chemmater.3c02482.

(35) Kuroda, K.; Ishizawa, N.; Mizutani, N.; Kato, M. The crystal structure of α-$SrMnO_3$. *Journal of Solid State Chemistry* **1981**, *38* (3), 297-299. DOI: 10.1016/0022-4596(81)90059-1.

(36) Grey, I. E.; Li, C.; Cranswick, L. M. D.; Roth, R. S.; Vanderah, T. A. Structure Analysis of the 6H–Ba(Ti, Fe^{3+}, Fe^{4+})$O_{3-\delta}$ Solid Solution. *Journal of Solid State Chemistry* **1998**, *135* (2), 312-321. DOI: 10.1006/jssc.1997.7652.

(37) Boullay, P.; Hervieu, M.; Labbé, P.; Raveau, B. Single crystal and HREM study of the "Bi-Sr" stabilized $BaMnO_3$ 9R polytype. *Materials Research Bulletin* **1997**, *32* (1), 35-42. DOI: 10.1016/s0025-5408(96)00169-9.

(38) Choy, J.-H.; Hong, S.-T.; Jae-Hyun Park, J.-H. P.; Dong-Kuk Kim, D.-K. K. Crystal Structure and the Role of Covalency in Eight-Layered Hexagonal Ba_2CrTaO_6. *Japanese Journal of Applied Physics* **1993**, *32* (10R). DOI: 10.1143/jjap.32.4628.

(39) Potoff, A. D.; Chamberland, B. L.; Katz, L. A single crystal study of eight-layer barium managanese oxide, $BaMnO_3$. *Journal of Solid State Chemistry* **1973**, *8* (3), 234-237. DOI: 10.1016/0022-4596(73)90090-x.

(40) Battle, P. D.; Davison, C. M.; Gibb, T. C.; Vente, J. F. Structural chemistry of $SrMn_{1-x}Fe_xO_{3-\delta}$, x≈ 0.3. *J. Mater. Chem.* **1996**, *6* (7), 1187-1190. DOI: 10.1039/jm9960601187.

(41) Vente, J. F.; Battle, P. D. Structural Chemistry and Electronic Properties of the Hexagonal Perovskites $BaIr_{1-x}Co_xO_{3-\delta}$ (x=0.5, 0.7, 0.8). *Journal of Solid State Chemistry* **2000**, *152* (2), 361-373. DOI: 10.1006/jssc.2000.8664.

(42) Adkin, J. J.; Hayward, M. A. $BaMnO_{3-x}$ Revisited: A Structural and Magnetic Study. *Chemistry of Materials* **2007**, *19* (4), 755-762. DOI: 10.1021/cm062055r.

(43) Liu, G.; Greedan, J. E. Syntheses, Structures, and Characterization of 5-Layer $BaVO_{3-x}$ (x = 0.2, 0.1, 0.0). *Journal of Solid State Chemistry* **1994**, *110* (2), 274-289. DOI: 10.1006/jssc.1994.1170.

(44) Ehora, G.; Renard, C.; Daviero-Minaud, S.; Mentré, O. New $BaCoO_{3-\delta}$ Polytypes by Rational Substitution of O^{2-} for F^-. *Chemistry of Materials* **2007**, *19* (12), 2924-2926. DOI: 10.1021/cm070576o.

(45) Parras, M.; González-Calbet, J. M.; Alonso, J.; Vallet-Regí, M. Microstructural Characterization of $BaMnO_{3-y}$ ($0.08 \leq y \leq 0.12$): Evidence for a New Polytype (21R). *Journal of Solid State Chemistry* **1994**, *113* (1), 78-87. DOI: 10.1006/jssc.1994.1344.

(46) Togo, A.; Shinohara, K.; Tanaka, I. Spglib: a software library for crystal symmetry search. *ArXiv:1808.01590* **2018**. DOI: 10.48550/arXiv.1808.01590.

Supplementary Information for

“Hexagonal” Perovskites – From Stacking Sequence to Space Group Symmetry and New Opportunities

Sylvia L. Kunz[a], Michael Haefner[b], Oliver Clemens[a,*]

[a] University of Stuttgart, Institute for Materials Science, Materials Synthesis Group, Heisenbergstraße 3, 70569 Germany

* Corresponding Author:

Prof. Dr. Oliver Clemens

Email: oliver.clemens@imw.uni-stuttgart.de

Fax: +49 711 685 51933

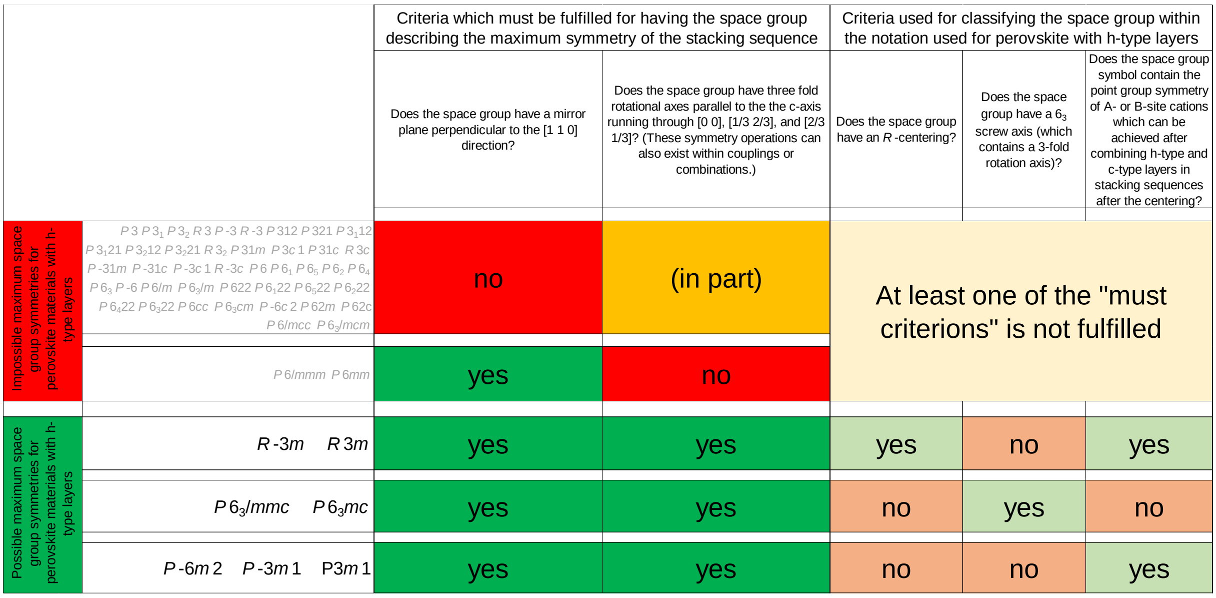

		Criteria which must be fulfilled for having the space group describing the maximum symmetry of the stacking sequence		Criteria used for classifying the space group within the notation used for perovskite with h-type layers		
		Does the space group have a mirror plane perpendicular to the [1 1 0] direction?	Does the space group have three fold rotational axes parallel to the the c-axis running through [0 0], [1/3 2/3], and [2/3 1/3]? (These symmetry operations can also exist within couplings or combinations.)	Does the space group have an *R* -centering?	Does the space group have a 6_3 screw axis (which contains a 3-fold rotation axis)?	Does the space group symbol contain the point group symmetry of A- or B-site cations which can be achieved after combining h-type and c-type layers in stacking sequences after the centering?
Impossible maximum space group symmetries for perovskite materials with h-type layers	$P3$ $P3_1$ $P3_2$ $R3$ P-3 R-3 $P312$ $P321$ $P3_112$ $P3_121$ $P3_212$ $P3_221$ $R3_2$ $P31m$ $P3c1$ $P31c$ $R3c$ P-$31m$ P-$31c$ P-$3c1$ R-$3c$ $P6$ $P6_1$ $P6_5$ $P6_2$ $P6_4$ $P6_3$ P-6 $P6/m$ $P6_3/m$ $P622$ $P6_122$ $P6_522$ $P6_222$ $P6_422$ $P6_322$ $P6cc$ $P6_3cm$ P-$6c2$ $P62m$ $P62c$ $P6/mcc$ $P6_3/mcm$	no	(in part)	At least one of the "must criterions" is not fulfilled		
	$P6/mmm$ $P6mm$	yes	no			
Possible maximum space group symmetries for perovskite materials with h-type layers	R-$3m$ $R3m$	yes	yes	yes	no	yes
	$P6_3/mmc$ $P6_3mc$	yes	yes	no	yes	no
	P-$6m2$ P-$3m1$ $P3m1$	yes	yes	no	no	yes

Figure S 1. Selection criteria which must be fulfilled for a space group symmetry to be a possible maximum symmetry for a perovskite-type material with h-type layers.

space group	**Orien-tation A/B/C/ α/β/γ**	**A in c-type layer with -3*m* symmetry**	**X in c-type layer with .2/*m*. symmetry**	**A in h-type layer with -6*m*2 symmetry**	**X in h-type layer with *mm*2. Symmetry** **A → x ≈ 0.5000** **B → x ≈ 0.1667** **C → x ≈ 0.8333**	**A in c/h-type layers with 3m symmetry**	**X in c/h-type layer with .*m*. symmetry** **A → x ≈ 0.5000** **B → x ≈ 0.1667** **C → x ≈ 0.8333**	**B with -3*m* symmetry**	**B with 3*m* symmetry**
R-3*m*	A / α	3*a* (0,0,0) 3*b* (0,0,$^{1}/_{2}$)	9*e* (0,$^{1}/_{2}$,0) 9*d* (0,$^{1}/_{2}$,$^{1}/_{2}$)			6*c* (0, 0, z)	18*h* (x, -x, z)	3*a* (0,0,0) 3*b* (0,0,$^{1}/_{2}$)	6*c* (0, 0, z)
*R*3*m*	A / α					3*a* (0, 0, z)	9*b* (x, -x, z)		3*a* (0, 0, z)
*P*6$_3$/*mmc*	A / α B / β C / γ	2*a* (0, 0, 0)	6*g* (0, $^{1}/_{2}$, 0)	2*b* (0, 0, $^{1}/_{4}$) 2*c* ($^{1}/_{3}$, $^{2}/_{3}$, $^{1}/_{4}$) 2*d* ($^{2}/_{3}$, $^{1}/_{3}$, $^{1}/_{4}$)	6*h* (x, -x, $^{1}/_{4}$) 6*h* (x, -x, $^{1}/_{4}$) 6*h* (x, -x, $^{1}/_{4}$)	4*e* (0, 0, z) 4*f* ($^{1}/_{3}$, $^{2}/_{3}$, z) 4*f* ($^{2}/_{3}$, $^{1}/_{3}$, z')	12*k* (x, -x, z) 12*k* (x, -x, z) 12*k* (x, -x, z)	2*a* (0, 0, 0)	4*e* (0, 0, z) 4*f* ($^{1}/_{3}$, $^{2}/_{3}$, z) 4*f* ($^{2}/_{3}$, $^{1}/_{3}$, z)
P-6*m*2	A / α B / β C / γ			1*a* (0,0,0) 1*d* ($^{1}/_{3}$,$^{2}/_{3}$,0) 1*f* ($^{2}/_{3}$,$^{1}/_{3}$,0) 1*b* (0,0,$^{1}/_{2}$) 1*d* ($^{1}/_{3}$,$^{2}/_{3}$,$^{1}/_{2}$) 1*f* ($^{2}/_{3}$,$^{1}/_{3}$,$^{1}/_{2}$)	3j (x,-x,0) 3j (x,-x,0) 3j (x,-x,0) 3k (x,-x,$^{1}/_{2}$) 3k (x,-x,$^{1}/_{2}$) 3k (x,-x,$^{1}/_{2}$)	2*g* (0, 0, z) 2*h* ($^{1}/_{3}$, $^{2}/_{3}$, z) 2*i* ($^{2}/_{3}$, $^{1}/_{3}$, z)	6*n* (x, -x, z) 6*n* (x, -x, z) 6*n* (x, -x, z)		2*g* (0, 0, z) 2*h* ($^{1}/_{3}$, $^{2}/_{3}$, z) 2*i* ($^{2}/_{3}$, $^{1}/_{3}$, z)
*P*6$_3$*mc*	A / α B / β C / γ					2*a* (0, 0, z) 2*b* ($^{1}/_{3}$, $^{2}/_{3}$, z) 2*b* ($^{2}/_{3}$, $^{1}/_{3}$, z)	6*c* (x, -x, z) 6*c* (x, -x, z) 6*c* (x, -x, z)		2*a* (0, 0, z) 2*b* ($^{1}/_{3}$, $^{2}/_{3}$, z) 2*b* ($^{2}/_{3}$, $^{1}/_{3}$, z)
P-3*m*	A / α B / β C / γ	1*a* (0,0,0) 1*b* (0,0,$^{1}/_{2}$)	3*e* (0,$^{1}/_{2}$,0) 3*f* (0,$^{1}/_{2}$,$^{1}/_{2}$)			2*c* (0, 0, z) 2*d* ($^{1}/_{3}$, $^{2}/_{3}$, z) 2*d* ($^{2}/_{3}$, $^{1}/_{3}$, z)	6*i* (x, -x, z) 6*i* (x, -x, z) 6*i* (x, -x, z)	1a (0,0,0) 1b (0,0,$^{1}/_{2}$)	2*c* (0, 0, z) 2*d* ($^{1}/_{3}$, $^{2}/_{3}$, z) 2*d* ($^{2}/_{3}$, $^{1}/_{3}$, z)
*P*3*m*	A / α B / β C / γ					1*a* (0, 0, z) 1*b* ($^{1}/_{3}$, $^{2}/_{3}$, z) 1*c* ($^{2}/_{3}$, $^{1}/_{3}$, z)	3*d* (x, -x, z) 3*d* (x, -x, z) 3*d* (x, -x, z)		1*a* (0, 0, z) 1*b* ($^{1}/_{3}$, $^{2}/_{3}$, z) 1*c* ($^{2}/_{3}$, $^{1}/_{3}$, z)

Table S 1. Overview of Wyckoff sites relevant to construct the aristotype symmetries of different Jagodzinski notations. Note that for R-centered space groups only the postion A/alpha is given, since every symmetry independent atom will appear in each orientation.

Details on the programming of the PerovGen computer programm

The only input required for the program PerovGen is a Jagodzinski sequence consisting of “c” and “h”, denoting a cubic and hexagonal ordering in the stacking sequence of the perovskite. The program automatically reduces and transforms the sequence to generate the smallest valid output structure. Using that sequence, it determines the space group, the stacking sequence in terms of layers A, B, and C and interlayers α, β, and γ, and which layers contain symmetry centers (inversion center or mirror plane perpendicular to stacking axis) of the associated perovskite. This information can be obtained with the “Info Structure” button. With the “Save Structure” button, the structure of the generated perovskite is standardized, using spglib [1], and saved as a CIF file with all relevant symmetry information for further processing with other programs.

In addition, the elements that comprise the perovskite can be customized according to the generalized perovskite formula ABX_3, where A indicates the A-site cation which formest he close packing together with the X anion, and B indicates the B-site cation in octahedral coordination by the X anions.

The source code and a compiled binary for Windows systems is available at https://github.com/mhaefner-chem/PerovGen [2].

References

(1) Togo, A.; Shinohara, K.; Tanaka, I. Spglib: a software library for crystal symmetry search. *ArXiv:1808.01590* **2018**. DOI: 10.48550/arXiv.1808.01590.

(2) Haefner, M. mhaefner-chem/PerovGen: PerovGen - v1.0.0 (v1.0.0). *Zenodo* **2024**. DOI: 10.5281/zenodo.12165868.